Study of the physical and functional interaction between Mog1 and Histones

UNIVERSITAT POLITÈCNICA DE VALÈNCIA

ESCOLA TÈCNICA SUPERIOR D'ENGINYERIA AGRONÒMICA I DEL MEDI NATURAL

GRADO EN BIOTECNOLOGÍA

Mª DOLORES SERRANO MARTÍN

TUTOR: JOSÉ RAMÓN MURGUÍA IBÁÑEZ

COTUTORA: SUSANA RODRÍGUEZ NAVARRO

COTUTOR COLABORADOR: JOAN SERRANO QUÍLEZ

Curso Académico: 2019-2020

Valencia, marzo 2020

Study of the physical and functional interaction between Mog1 and Histones

Mog1 was first described as a Gsp1-binding protein involved in nuclear protein import both in humans and yeast, being Gsp1 the homologue of the human Ran-GTPase. Later, it was found that human Mog1 also regulates the traffic of $Na_v1.5$, the α-subunit of the cardiac sodium channel, that has been associated with Brugada syndrome, a cardiac disease. Recently, it has been discovered that Mog1 regulates mRNA transcription and export to the cytoplasm in *Saccharomyces cerevisiae* by participating in the establishment of epigenetic marks during transcription, specifically H2B monoubiquitylation on lysine 123 (H2Bub1) and H3 trimethylation on lysine 4 (H3K4me3). These post-translational modifications (PTMs) are correlated with actively transcribed genes, being important for transcription elongation, amongst other functions. In addition, there is a crosstalk between H2Bub1 and H3K4me3 since H2Bub1 has been shown to stimulate H3K4me3. However, the exactly molecular mechanism explaining why these PTMs enhance transcription is not fully understood, although some mechanisms have been proposed in which several proteins and complexes are involved.

How Mog1 participate in this process is unknown but it was proposed that it is independent on its role in Gsp1 binding, suggesting the existence of two cellular pools of Mog1 protein. Moreover, it has been shown that two subunits of the COMPASS complex, Shg1 and Sdc1, and histones H2B1, H3 and H4, amongst other proteins, co-precipitate with Mog1-Tap tagged. The interaction between Shg1 and Mog1 has been validated through a genome wide Shg1 two-hybrid screening, finding a region in Mog1 between amino acids residues 114 and 154 as the putative binding domain. Part of this region is located in a long loop connecting two beta sheets where there is a tryptophan residue at position 145 especially exposed. Therefore, it is interesting to study if this loop and, especially, W145 are important for Mog1-Shg1 binding.

On the other hand, Mog1 co-immunoprecipitation with histones H2B1, H3 and H4 revealed that Mog1 could participate in the establishment of H2Bub1 and H3K4me3 by directly or indirectly binding histones. Of especial interest is H2B because of H3-K4 trimethylation dependency on H2B-K123 monoubiquitylation. Consequently, it is important to clarify if Mog1 interacts with H2B directly and if so, to determine the interaction domain.

Furthermore, it was found in a screening that lysine at position 189 in Mog1 can be ubiquitylated which points Mog1 as a putative substrate for posttranslational modifications.

Therefore, the main objective of this study is to gain knowledge about the role of Mog1 in the modulation of histone epigenetic modifications H2Bub1 and H3K4me3 by, on the one hand, analysing the phenotypic effect of several Mog1 mutants and, on the other hand, characterising histone H2B-Mog1 interaction.

Keywords: *MOG1*, mRNA transcription, posttranslational modifications, histones, H2Bub1, H3K4me3, *SHG1*

Author: Mª Dolores Serrano Martín

Valencia, March 2019

Tutor: José Ramón Murguía Ibáñez PhD

Co-tutor: Susana Rodríguez Navarro PhD

Contributing co-tutor: Joan Serrano Quílez

Estudio de la interacción física y funcional entre Mog1 e Histonas

Mog1 fue descrita por primera vez como una proteína de unión a Gsp1, proteína homóloga a Ran-GTPasa en humanos, que participa en la importación de proteínas al núcleo tanto en levadura como en humanos. Más tarde, se encontró que, en humanos, Mog1 regula el tráfico de $Na_v1.5$, la subunidad α del canal de sodio cardiaco, que ha sido asociada con el síndrome de Brugada, una enfermedad cardiaca. Recientemente, se ha descubierto que Mog1 también regula la transcripción y exportación del ARNm en *Saccharomyces cerevisiae* mediante la participación en el establecimiento de marcas epigenéticas durante la transcripción. Estas modificaciones postraduccionales (PTMs por sus siglas en inglés) son la monoubiquitinación de H2B en la lisina 123 o H2Bub1 y la trimetilación de la histona H3 en la lisina 4 o H3K4me3 que están relacionadas con genes activamente transcritos y son importantes en la elongación transcripcional, entre otras funciones. Además, existe una intercomunicación entre H2Bub1 y H3K4me3 ya que se ha demostrado que H2Bub1 estimula la trimetilación de H3 en K4. Sin embrago, no se ha caracterizado todavía un mecanismo molecular que explique por qué estas PTMS aumentan la transcripción, aunque varios mecanismos se han propuesto englobando varias proteínas y complejos.

Se desconoce cómo Mog1 participa en este proceso, pero se ha propuesto que esta función es independiente a su unión a Gsp1, sugiriendo la existencia de dos *pools* celulares de Mog1. Además, se ha encontrado que dos subunidades del complejo COMPASS, Shg1 y Sdc1, y las histonas H2B1, H3 y H4, entre otras proteínas, coprecipitan en un ensayo con Mog1 con cola Tap. La interacción entre Mog1 y Shg1 ha sido validada en un ensayo de doble híbrido empleando Shg1 como la proteína *bait*, en el que además se describió una región en Mog1 entre los aminoácidos 114 y 154 como posible dominio de interacción. Parte de esta secuencia está localizada en una región de bucle que conecta dos láminas beta y que contiene un triptófano en posición 145 con su cadena lateral especialmente expuesta. Por lo tanto, es interesante estudiar si esta región de bucle y, en concreto, W145 son importante para la interacción entre Mog1 y Shg1.

Por otra parte, la co-inmunoprecipitación de Mog1 e histonas H2B1, H3 y H4 sugiere que Mog1 podría desempeñar su función en el establecimiento de H2Bub1 y H3K4me3 interaccionando directa o indirectamente con las histonas. H2B es de especial interés por su influencia en la trimetilación de H3 en K4. Por ello, es importante estudiar si Mog1 interacciona con H2B directamente y en tal caso, determinar el dominio de interacción.

Además, un estudio ha encontrado que la lisina 189 en Mog1 puede estar ubiquitinada, indicando que Mog1 también puede ser sustrato para las modificaciones postraduccionales.

En consecuencia, el objetivo principal del presente estudio es indagar en la implicación de Mog1 en el establecimiento de las marcas epigenéticas H2Bub1 y H3K4me3 mediante el análisis del efecto fenotípico de varias mutaciones en la proteína Mog1, y la caracterización de la interacción entre la histona H2B y Mog1.

Palabras clave: *MOG1,* transcripción, modificaciones postraduccionales, histonas, H2Bub1, H3K4me3, *SHG1*

Autor: Mª Dolores Serrano Martín

Tutor: Dr. José Ramón Murguía Ibáñez

Cotutora: Dra. Susana Rodríguez Navarro

Cotutor colaborador: Joan Serrano Quílez

Acknowledgements

En primer lloc, vull agrair a tots els meus companys i companyes del laboratori d'Expressió Gènica i Metabolisme del RNA o UEG/ I-25, segons el matràs/proveta que trobes: Ana, Joan, Carme, Jesús, Clara, Lolo, JR i Susana. Gràcies per tractar-me com una més des del primer dia i convidar-me a tots els plans des de dinars i sopars, passant per senderisme i esmorzaret, fins a concursos de pòsters i postres. Però sobretot gràcies per haver-me ensenyat tantíssim de ciència i, especialment, de treball en equip. Sou un gran grup! En especial, vull agrair a Susana per donar-me la oportunitat de formar part del seu equip i per confiar en mi i a Joan per ajudar-me pacientment en tot el que he necessitat.

En segon lloc, gràcies a tots els meus amics i amigues perquè heu tingut temps per dedicar-me una estona quan ho he necessitat: *Friends shore*, els de tota la vida; *Tomacos y Cítricos*, els del Colmadito i el Viñedo; las *Polifacéticas*, les que em fan riure sense parar.

En tercer lloc, gràcies a tota la meua família per recolzar-me incondicionalment sempre. En especial, als meus pares, iaios i la meua germana per transmetre'm tanta força i ser el meu exemple a seguir. I com no, a Marco per tindre sempre una abraçada preparada.

Index

Figure list

Table list

Abbreviation list

aa	Amino acid
Amp	Ampicillin
APS	Ammonium persulfate
bp	Base pair
BSA	Bovine Serum Albumin
ChIP	Chromatin immunoprecipitation
Chl	Chloramphenicol
COMPASS	Complex of proteins associated with Set1
CV	Column volume
DNA	Deoxyribonucleic acid
DUBm	DeUbiquitilating module
EDTA	Etilendiaminotetraacetic acid
IPTG	Isopropyl β-D-1-thiogalactopyranoside
Kan	Kanamycin
LB	Luria-Bertani medium
MATa	Mating a
mRNA	Messenger RNA
nt	Nucleotide
NUP	Nuclear Pore Complex
o/n	Overnight
OD_{600}	Optical density 600nm
ORF	Open Reading Frame
PBS	Phosphate buffered saline
PCR	Polymerase chain reaction
PEG	Polyethylene glycol
RNA	Ribonucleic acid
RNAPII	RNA polymerase II
SAGA	Spt-Ada-Gcn5 acetyltransferase
SC	Synthetic complete medium
SDS	Sodium dodecyl sulfate
SDS-PAGE	SDS polyacrylamide gel electrophoresis
SRN	Susana Rodríguez Navarro
TAE	Tris-acetate EDTA
TAP	Tandem Affinity Purification
TBS	Tris-Buffered Saline
TCA	Trichloroacetic acid
TE	Tris-EDTA
TEMED	Tetramethylethane-1,2-diamine
v/v	Volume/volume
w/v	Weight/volume
WT	Wild type
YNB	Nitrogen base for yeast
YPD	Yeast extract-peptone-dextrose

1. INTRODUCTION

Saccharomyces cerevisiae, commonly known as budding yeast, is a type of yeast and one of the simplest eukaryotic organisms consisting of a nucleated single cell. This means that it shares biological properties with other eukaryotic organisms, but its genetic manipulation is easier compared to more complex animal models. In addition, it became the first eukaryotic organism to have its genome completely sequenced in 1996 (Goffeau et al. 1996), with its first major update in 2010 (Otero et al. 2010), being this information available and manually curated in the Saccharomyces genome database (Cherry et al. 2012). In addition, the large-scale international Yeast Consortium 2.0 is currently constructing a synthetic version of the genome of the BY lineage of the SC288C reference strain likely being the first synthetic eukaryotic genome (SYNTHETIC YEAST 2.0, 2020). Because of the availability of its genetic information, the easy growth and manipulation and the powerful genetic techniques developed, *S. cerevisiae* has been widely used as a model organism to study different biological processes such as aging, regulation of gene expression, signal transduction, cell cycle and apoptosis (Karathia et al. 2011). Of especial interest is the use of budding yeast to study evolutionary conserved protein complexes (Cherry et al. 2012) since its representativeness has been supported by functional homology studies. One of these studies found statistically robust homologs of 31% of all the protein-encoding genes of yeast amongst the mammalian protein sequence (Botstein et al. 1997). Another work performed by Foury (1997) showed that 30% of the genes involved in human diseases have orthologs in the yeast proteome.

One of these orthologous genes is the one encoding the Mog1 protein, which was first identified in yeast. Yeast Mog1p is a 24kDa nuclear protein encoded by the yeast ORF *YJR074W* that binds Gsp1p, the *S. cerevisiae* orthologue of the human Ran GTPase, which is essential for the nucleocytoplasmic exchange of macromolecules through the nuclear pore complex (NPC) (Oki and Nishimoto, 1998). Mog1 binds to both nucleotide states of Gsp1, acting as a guanine nucleotide release factor together with RanGEF but remaining bound to the nucleotide-free Ran in contrast to RanGEF (Steggerda and Paschal, 2000). Later, it was found that Mog1 induces nucleotide release by blocking the GTPase active site (Steggerda and Paschal, 2001). However, Mog1p has been only related to protein import but not to protein export (Oki and Nashimoto, 1998; Baker et al. 2001). The 1.9Å resolution crystal structure of the yeast Mog1p was solved by Steward and Baker (2000) (Figure 1.1.A). which helped to find a cluster of highly conserved surface residues by analysing sequences of Mog1p homologues. This cluster was located between amino acids 25 and 190 with the highest homology between residues 38 and 67 which were indicative of a putative Ran binding site. Later they identified by mutagenesis the conserved acidic surface residue Glu65 of Mog1p as an important player in maintaining the Mog1-Ran interaction since Mog1-E65K mutant showed defects in nuclear protein import (Baker et al. 2001). As other proteins mediating nuclear transport, Mog1p has been structurally and functionally conserved throughout evolution, finding an orthologue in humans, encoded by the *RANGRF* gene. Human Mog1p is a nuclear 28kDa protein that binds to both yeast and human Ran GTPase complex and has a role in nuclear protein import as yeast Mog1p (Marfatia et al. 2001). Its structure was also solved by Bao et al. (2018) (Figure 1.1.B).

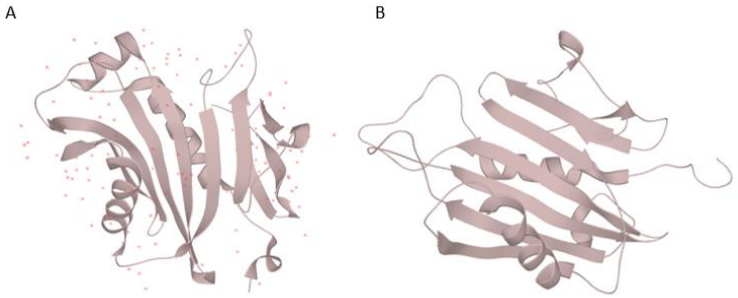

Figure 2.1. Yeast and human Mog1 structure. *A) X-ray diffraction 1.9Å resolution crystal structure of the yeast Mog1p solved by Steward and Baker (2000). B) NMR solution structure of the human Mog1p solved by Bao et al. (2018). Images from UniProtKB (UNIPROT CONSORTIUM, 2019).*

Later, it was found that human Mog1p could have a role in Brugada syndrome, a heart disease first described in 1992 (Brugada and Brugada, 1992), which is characterized by an irregular electrocardiographic pattern and it is responsible for 4-12% of the cases of sudden death and ≈20% of death in patients with no structural cardiopathies (Antzelevitch et al. 2002). At the beginning, it was thought to be a genetic disorder due to autosomal dominant mutations in the *SCN5A* gene which codifies for $Na_v1.5$, the α-subunit of cardiac sodium channel. Up to 100 mutations have been identified in this gene, all of them leading to a lower transmembrane sodium current (Chen et al. 1998, Smits et al. 2002). However, only 18-30% of the patients present mutations in this gene, suggesting the implication of other genes or proteins (Antzelevitch et al. 2005). One of these proteins is Mog1 which was found to interact with the cytoplasmatic loop II of $Na_v1.5$ and to increase the cell surface expression of the channel (Wu et al. 2008). Later studies showed that Mog1 promotes intracellular trafficking of $Na_v1.5$ to plasma membranes in cardiomyocytes (Kattygnarath et al. 2011) and the interaction domain was suggested to be located in Mog1 from 146 to 155aa, which corresponds to a long loop in the human Mog1 structure (Yu et al. 2018).

Recently, a new function of Mog1p in mRNA transcription and export has been described in yeast. This is related to the participation of Mog1p in the establishment of epigenetic marks during transcription, specifically in H2B monoubiquitylation on lysine 123 (H2Bub1) and H3 trimethylation on lysine 4 (H3K4me3) (Oliete-Calvo et al. 2018). In the eukaryotic nucleus, DNA is packaged by wrapping DNA around a globular histone octamer named nucleosome, which is formed by two dimers of histone H2A/H2B and a tetramer of H3/H4 (Kornberg and Lorch, 1999). Since the early 1960s it is known that histones present post-translational modifications (PTMs) (Allfrey et al. 1964), which were localized in basic amino-terminal tails protruding from the histones when the structure of the nucleosome was solved by X-ray crystallography in 1997 (Luger et al 1997a). Why these PTMs are important for chromatin structure regulation is not only due to its exposed position within the nucleosome, but also because they are able to be recognized by remodelling enzymes. However, the function of PTMs goes beyond chromatin structure remodelling, being involved in many other DNA processes such as transcription, repair, replication and recombination (Bannister and Kouzarides, 2011). Amongst the different PTMs that have been described, histone methylation and ubiquitylation are of special interest for our study. Histone methylation consists in the addition of one, two or three methyl groups on the side chains of lysine and arginine residues, becoming mono-, di- or tri-methylated. It is a dynamic modification, being "written" by histone methyltransferases and "erased" by demethylases and produces relatively small molecular changes to the amino acid side chains (Klose and Zhang, 2007). In contrast, histone ubiquitylation is a much larger covalent modification resulting in the attachment of ubiquitin, a 76-amino acid polypeptide, to lysine residues on histone tails. This is performed by the co-operative and sequential action of three proteins: E1-activating, E2-conjugating and E3-ligating enzymes (Hershko and Ciechanover, 1998). As in the case of methylation, this modification can be removed by de-ubiquitin enzymes and the degree of ubiquitylation changes from mono- to poly-ubiquitylated being mono-ubiquitylation the most relevant for gene expression (Wang et al. 2004).

Consequently, gene expression is not only regulated by genetic factors, but also by those that are epigenetic. Complexity increases because of the recruitment of multivalent proteins and complexes to these PTMs through specific domains (Bartke et al. 2010). This is even more complex when considering the crosstalk between different modifications resulting in the overall

control of gene expression. This crosstalk can occur (1) because of competitive antagonism between modifications targeting the same site; (2) because the establishment of one modification is dependent on another one; (3) by disrupting the binding of a protein to a particular modification by an adjacent modification or (4) because several modifications might be necessary for the recruitment of specific factors on adjacent modifications (Kouzarides, 2007).

H2Bub1 and H3K4me3 modifications exemplify this intricate mechanism and are both correlated with actively transcribed genes playing a role in transcription elongation (Kouzarides, 2007). On the one hand, it is known that H3K4me3 localizes to the 5' end of actively transcribed genes in budding yeast (Kouzarides, 2007; Berger, 2007). On the other hand, H2Bub1 and its homologue in humans H2B-K120 monoubiquitylation (Osley, 2006) is an essential histone modification for optimal gene transcription (Pavri et al. 2006) and mRNA export (Vitaliano-Prunier et al. 2012), apart from participating in DNA damage response (Giannattasio, 2005) and DNA replication (Trujillo and Osley, 2012). Nevertheless, the molecular mechanism by which these modifications enable transcription elongation is still unknown. In yeast, H2B monoubiquitylation is catalysed by both the ubiquitin conjugating enzyme Rad6 (E2) and the ubiquitin ligase enzyme Bre1 (E3) together with the transcriptional regulatory protein Lge1 (Osley, 2006), while it is deubiquitylated by two ubiquitin-specific proteases, Ubp8 and Ubp10 (Henry et al. 2003; Ingvarsdottir et al. 2005). Studies found that both monoubiquitylation and deubiquitylation are required for gene transcription, being an important checkpoint for transcription elongation (Henry et al. 2003, Wood et al. 2003; Pavri et al. 2006; Lee et al. 2007). Why H2Bub1 is important in mRNA transcription elongation might be explained by the interaction of Rad6 and Bre1 with Paf1 C and the FACT complex (Figure 1.2) (Weake and Workman, 2008; Thornton et al. 2014). The Paf1 C (Polymerase-Associated Factor 1 complex) was initially described as a regulator in all the stages of the Pol II transcription cycle (Squazzo et al. 2002; Rondón et al. 2004). It was found that Rtf1, a subunit of Paf1C (Mueller and Jaehning, 2002), directly promotes H2B monoubiquitylation on K123 by interacting with Rad6 and stimulating its activity (Ng et al. 2003; Wood et al. 2003, Van Oss et al. 2016). In addition, it has been shown to interact with RNA polymerase II in yeast (Shi et al. 1996). On the other hand, it has been suggested that H2Bub1 assists the recruitment of the histone chaperone FACT (Facilitates Chromatin Transcription) which participates in transcription elongation by binding to RNA polymerase II and displacing H2B/H2A heterodimers to allow its passage (Pavri et al. 2006; Fleming et al. 2008). Moreover, Paf1C and FACT have been shown to genetically and physically interact in yeast (Formosa et al. 2002). Altogether, these findings show that H2BK123 is monoubiquitylated co-transcriptionally and H2Bub1 levels have been related with RNAPII elongation rate (Fuchs and Oren, 2014).

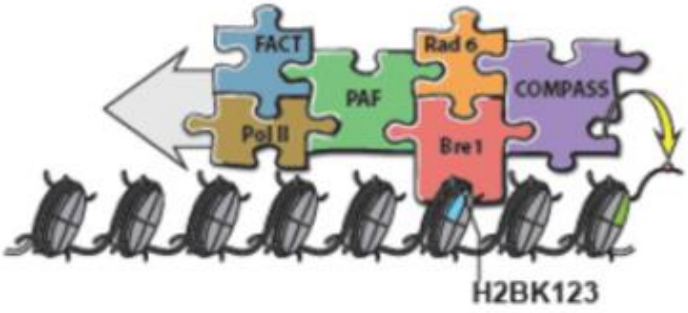

Figure 1.2. Molecular mechanism proposed by Thornton et al. (2014) that explains FACT and Paf1C interaction with the H2B ubiquitylation machinery in the context of transcription elongation.

Other studies showed that the disruption of either ubiquitylation or Ubp8-mediated deubiquitylation of H2B leads to changes in di- and trimethylation of H3K4, potentially being an example of the trans-regulation process between PTMs described previously (Wood et al. 2003; Shahbazian et al. 2005; Lee et al. 2007). Why this crosstalk happens between H2Bub1 and H3K4me3 has been widely studied and several mechanisms have been proposed, most of them pointing Swd2 as the main element in H2Bub1-H3K4me3 crosstalk (Lee et al. 2007, Zheng et al. 2010; Soares and Buratowski, 2012). Swd2 is a subunit within the macromolecular complex COMPASS (Complex of Proteins Associated with Set1), which is composed by other seven subunits highly conserved in eukaryotes: Set1, Bre2, Swd1, Spp1, Swd3, Sdc1 and Shg1 (Miller et al. 2001). Set1 is the enzyme that catalyses H3K4 mono-, di- and trimethylation (Miller et al. 2001; Krogan et al. 2002; Shilatifard, 2012). In 2008, Vitaliano-Prunier et al. (2008) showed that the recruitment of Rad6 and Bre1 to H2BK123 leads to ubiquitylation not only of H2BK123 but also of Swd2 on Lys68 and Lys69. Upon ubiquitylation, Swd2 becomes able to recruit Spp1 to the chromatin, which is the subunit of COMPASS required for H3K4 di- and trimethylation from the monomethylated state (Morrillon et al. 2005, Dehé et al. 2006). Therefore, H2Bub1-dependent Swd2 ubiquitylation would allow the efficient recruitment of the complete and stable form of the COMPASS complex (Figure 1.3), being this mechanism conserved in mammals, including humans (Kim et al. 2009). H2Bub1 also promotes Dot1-dependent H3K79 methylation (Vlaming and van Leeuwen, 2016) and Set2-mediated H3K36 methylation (Hérissant et al. 2014); but since the loss of *MOG1* did not affect global levels of H3K79me3 and H3K36me3 (Oliete-Calvo et al. 2018), these histone crosstalks will not be covered in this work.

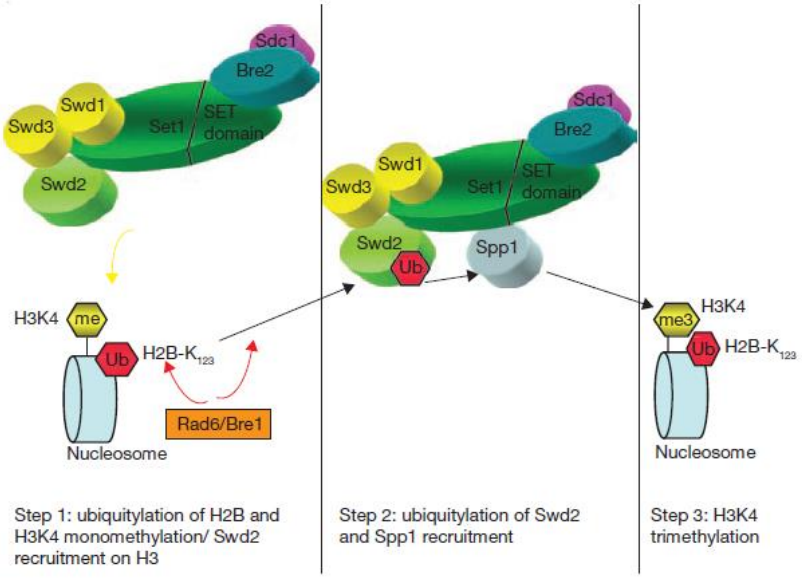

Figure 1.3. Molecular mechanism for H2Bub1-H3K4me3 crosstalk proposed by Vitaliano-Prunier et al. (2008). *Shg1 is not showed in this graph.*

Consequently, monoubiquitylation/deubiquitylation and trimethylation/demethylation of H2BK123 and H3K4 respectively, are complex biological processes in which several proteins and complexes participate interacting with each other and with chromatin. The role of Mog1p in this mechanism was first suggested when Mog1 was found to genetically interact with the DUBm (DeUbiquitilating module) subunits Ubp8 and Sus1 (Köhler et al. 2006; Shukla et al. 2006). This led to the conclusion that Mog1p and Ubp8/Sus1 may participate in the same biological process. To answer this question, Oliete-Calvo et al. (2018) checked H2Bub1 and H3K4me3 levels in *S. cerevisiae* cells lacking *MOG1*, being these significantly reduced compared to the wild type strain. To unravel why Mog1p could modulate H2Bub1 and H3K4me3 levels, Oliete-Calvo et al. (2018)

combined *mog1Δ* with deletion of proteins participating in H2B monoubiquitylation and H2Bub1-H3K4me3 crosstalk such as *RAD6*, *BRE1*, *LGE1* and *RTF1*. These double mutants showed an additive growth phenotype compared to individual mutants leading to the conclusion that Mog1 and Rad6, Bre1, Lge1 or Rtf1 act in independent pathways. In addition, they analysed the growth of *mog1Δ* cells with mutations in H2B (H2B-K123R) and H3 (H3-K4A) specifically defective in H2B monoubiquitylation and H3 trimethylation, respectively. These yeast strains showed a subtle growth retardation suggesting the implication of Mog1p in other pathways other than H2B monoubiquitylation and H3 trimethylation. However, since Mog1p participates in nuclear protein import (Oki and Nishimoto, 1998; Marfatia et al. 2001), these effects of *MOG1* deletion on growth could be due to disruption of nuclear import of proteins participating in H2BK123 monoubiquitylation. This possibility was examined by Oliete-Calvo et al. (2018) by tagging Rad6, Bre1, Rtf1 and Ubp8 with GFP and monitoring their cellular localization in both *mog1Δ* and WT yeast cells finding that in both cases, these proteins localized in the nucleus. These results showed that the nuclear protein import disruption was not responsible for low levels of H2Bub1 and H3me3, which indeed suggests the existence of two different pools of Mog1p in the cell, one participating in nuclear protein import and the other in the regulation of gene transcription and mRNA export.

Once it was clear that Mog1p participates in the establishment of H2Bub1 and H3K4me3 and according to previous studies showing the role of H2Bub1 in transcription and mRNA export (Pavri et al. 2006; Bannister and Kouzarides, 2011), the question to assess was if *MOG1* deletion affected transcription levels and mRNA export. Oliete-Calvo et al. (2018) showed that global levels of mRNA synthesis rate (SR) and mRNA abundance (RA) were significantly lower (25% reduction for SR and 30% in case of RA) in *mog1Δ* compared to wild type yeast cells. Furthermore, the deletion of *MOG1* led to inefficient mRNA export at 39ºC when compared to WT. Therefore, the remaining question was how Mog1p affected H2B monoubiquitylation and H3K4 trimethylation. Oliete-Calvo et al. (2018) performed ChIP experiments to study chromatin recruitment of Rad6, Bre1 and Rtf1 in the 3' and 5' coding regions of actively transcribed genes (*ADH1*, *PMA1* and *YEF3*) in *mog1Δ* and wild type cells. Results showed that the overall gene association of these factors was significantly lower in *mog1Δ* cells specially in 5'ORF finding in Rtf1 the strongest effect. Consequently, they TAP-tagged Mog1 in a yeast strain expressing Rtf1-Pk, finding that immunoprecipitation of Mog1-TAP co-precipitated Rtf1-PK, which may be indicative of direct or indirect physical contact between these two proteins.

Nevertheless, not only does Rtf1 interact with Mog1. Immunoprecipitation of TAP-tagged Mog1 and mass spectrometric analysis (LC/MS-MS) revealed that apart from its previously described partners, the GTP-binding proteins Gsp1, Gsp2, Nop1 and Lgs1 (Oki and Nishimoto, 1998; Baker et al. 2001); the ligase Bre1; Spt5; fourteen subunits of the SAGA complex; two subunits of the COMPASS complex (Shg1 and Sdc1); histones H2B1, H3 and H4; and several NUPs co-purified with Mog1(Oliete-Calvo et al. 2018). From these proteins, Shg1 is of special interest for several reasons: (1) the interaction between Shg1 and Mog1 was validated trough a genome wide Shg1 yeast two-hybrid screening finding a region between nucleotides 342 and 464 (between aa residues 114 and 154) in all identified Mog1 clones through which they interacted with Shg1 (Oliete-Calvo et al. 2018); (2) although Shg1 was described as an additional subunit of yeast COMPASS (Roguev et al. 2001), no mammalian homologues have been yet identified and it does not seem to have any effect over the pattern of H3K4 methylation by itself (Mueller et al. 2006), therefore, its role might be allowing the interaction between Mog1 and COMPASS; (3) When analysing the possible interaction domain between Mog1 and Shg1 in the crystal structure of Mog1 (Stewart and Baker, 2000), it is interesting to notice that residues 143 to 154 are located in an exposed loop connecting two beta sheets (Figure 1.4.A). Amongst these 11 aa there is a tryptophan residue at position 145 with its side chain projecting away from the rest of the residues

forming the loop (Figure 1.4.B). Since this residue is significantly exposed it is interesting to study if it is important for Shg1-Mog1 binding.

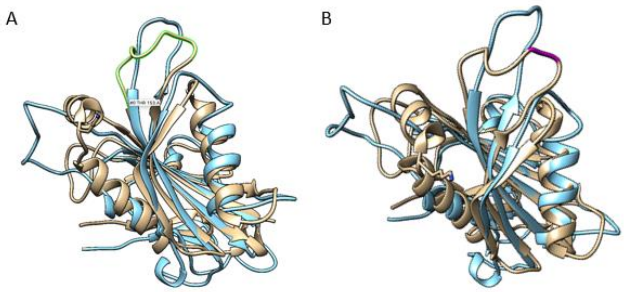

Figure 1.4. Yeast Mog1 protein structure (brown) and human Mog1 structure (blue) overlapped. *A) Part of the putative Shg1-Mog1 interaction domain highlighted in yellow in yMog1. Exposed loop connecting two beta sheets. B) W145 highlighted in purple in yMog1 inside the loop containing part of the putative interaction domain between Mog1 and Shg1. Images obtained from UCSF Chimera software (Pettersen et al. 2004).*

This new role of Mog1 in H2B monoubiquitylation and H3K4 methylation was suggested to be independent of Mog1 function in nuclear protein import (Oliete-Calvo et al. 2018). In *mog1Δ* transformed with the Ran binding mutant Mog1-E65K (Figure 1.5A), methylation and ubiquitylation levels recovered the ones showed by *mog1Δ* yeast cells what, therefore, supports the hypothesis of the two cellular pools of Mog1. In this line of research and considering the likely participation of Mog1 residue W145 in Shg1-Mog1 interaction, it is reasonable to think that modifying both residues (E65 and W145) Mog1 function will be impaired both in nuclear protein import and mRNA transcription and export. Moreover, Swaney et al. (2013) found in a screening of proteins ubiquitylated and/or phosphorylated in *S. cerevisiae* that the lysine at position 189 in Mog1 (Figure 1.5B) is ubiquitylated showing that Mog1 is not only a player in the establishment of histone modifications but also a putative substrate for posttranslational modifications.

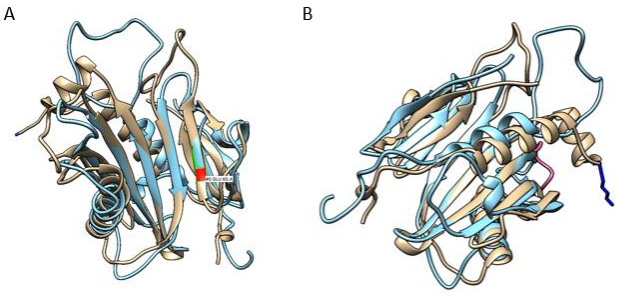

Figure 1.5. Yeast Mog1 protein structure (brown) and human Mog1 structure (blue) overlapped. A) *E65 residue highlighted in red in yMog1. B) K189 residue highlighted in blue in yMog1. Images obtained from UCSF Chimera software (Pettersen et al. 2004).*

Going back to Oliete-Calvo et al. (2018) results from immunoprecipitation of TAP-tagged Mog1 and mass spectrometry analysis, the interaction between Mog1 and histones H2B, H3 and H4 cannot be overlooked. The molecular mechanism by which Mog1 modulates H3K4me3 and H2Bub1 is unknown but these results suggest that Mog1 could perform this function by directly or indirectly contacting histones. Of special interest is H2B because on one hand, at the end it is affected by Mog1 function independently on the mechanism of action, and on the other hand, since H3K4me3 seems to depend on H2B monoubiquitylation it is likely that if Mog1 interacted with any histone, H2B would be the first one to be contacted. Therefore, and in the way of

answering the mechanism of action of Mog1 in epigenetic modifications, it is important to clarify if Mog1 interacts with H2B directly or indirectly. TAP-tag immunoprecipitations from cell extracts give important information on protein-protein interactions but these can be indirect since interacting proteins can be part of a larger complex or the interaction can proceed through another protein. This is particularly significant in the case of Mog1-H2B interaction since H2B is part of the histone octamer (Phizicky and Fields, 1995).

Consequently, interactions detected by this method should be counteracted by other *in vivo* or *in vitro* experiments. We could consider then other protein-protein interaction assays such as yeast two hybrid (*in vivo*) or affinity chromatography (*in vitro*). The yeast two hybrid system lies on the principle of using transcriptional activity to measure interaction since the DNA-binding domain of a transcriptional activator is fused to the N terminal of one of the proteins being studied and the transcriptional activation domain to the second protein. When both domains get close, the transcriptional activation is functional and stimulates the expression of a reporter gene that allows growth on a selective media or a colour reaction (Fields and Song, 1989). Therefore, the interaction is measured *in vivo* with the post-translational modifications naturally occurring in yeast. However, there are some disadvantages: fused proteins can avoid interactions because of steric hindrance leading to false negatives (Phizicky and Fields, 1995), false positives can arise because the fused transcriptional activation domain interacts with upstream activating sequences (Stephens and Banting, 2000) and it is limited to soluble proteins (Brücner et al. 2009). In addition, in our case the problem of identifying if Mog1 is indeed directly interacting with H2B or the other histones are mediating the interaction is still present. That is why affinity chromatography seems to be the best option for this approach. Testing the interaction of tagged proteins previously purified by affinity chromatography allows to determine direct interactions with a high sensitivity (Ratner, 1974; Phizicky and Fields, 1995) being essential for the representativeness of the results the purity of the proteins. In addition, when overexpressing the proteins in bacterial systems high protein yields and homogeneous protein extracts are obtained (Demain and Vaishnav, 2009). The main problems with this system are that proteins are not post-translationally modified and the possibility of losing their native structure during purification leading to false negatives (Phizicky and Fields, 1995). False negatives may also arise because of steric hindrance due to protein tags of large size which in contrast increase solubility and stability of the fused proteins (Lichty et al. 2005). These characteristics make affinity purification a good choice for studying Mog1-H2B interaction to support the results obtained by Oliete-Calvo et al. (2018) having the limitations of this technique in mind.

2. OBJECTIVES

With the aim of understanding the role of Mog1 in the modulation of histone epigenetic modifications H2Bub1 and H3K4me3, and in the context of the physical and functional interactions between Mog1 and other proteins and complexes involved in the establishment of these modifications, the main objectives of this project are:

1. Analyse the phenotypic effect of the W145A single and E65KW145A double Mog1 mutants on their ability to restore the growth of *mog1Δ* and *set1Δmog1Δ S. cerevisiae* strains.
2. Analyse the phenotypic effect of the deletion of the K144-T153 region of Mog1 and preventing ubiquitylation of K189 in Mog1 by alanine substitution on their ability to restore the growth of *mog1Δ* and *set1Δmog1Δ S. cerevisiae* strains.
3. Study the *in vitro* direct interaction between H2B and Mog1 by affinity chromatography using a bacterial expression system.
4. Study the *in vitro* direct interaction between H2B and the shorter version of Mog1, $Mog1_{78\text{-}218}$, lacking the Gsp1 binding domain, by affinity chromatography using a bacterial expression system.

3. MATERIALS AND METHODS

3.1. Yeast and bacterial strains, growth media, plasmids, antibodies and primers used

All the yeast and bacterial strains, growth media, plasmids, antibodies and primers used during the experiments are listed in the following tables together with complementary information.

Table 3.1. Yeast strains used, their selection markers and origin or reference.

Strain	Genotype	Origin/Reference
BY4741 (WT)	MATa *his3Δ1 leu2Δ0 met15Δ0 ura3Δ0*	Winston et al. 1995
mog1Δ	MATa *his3Δ1 leu2Δ0 met15Δ0 ura3Δ0 mog1::HIS3*	This group
set1Δ	MATa *his3Δ1 leu2Δ0 met15Δ0 ura3Δ0 set1::KANMX4*	EUROSCARF (collection from 2004)
set1Δmog1Δ	MATa *his3Δ1 leu2Δ0 met15Δ0 ura3Δ0* set1*::KANMX4 mog1::HIS3*	This work, created from *set1Δ* strain.

Table 3.2. Bacterial strains used, their selection marker and origin or reference.

Strain	Genotype	Origin/Reference
DH5α competent *Escherichia coli*	dlacZ Delta M15 Delta(lacZYA-argF) U169 recA1 endA1 hsdR17(rK-mK+) supE44 thi-1 gyrA96 relA1	Hanahan, 1983
BL21-CodonPlus (DE3) E*scherichia coli*	fhuA2 [lon] ompT gal (λ DE3) [dcm] ΔhsdS λ DE3 = λ sBamHIo ΔEcoRI-B int: :(lacI::PlacUV5::T7 gene1) i21 Δnin5	Wood, 1966
DH5α electrocompetent *Escherichia coli*	fhuA2Δ(argF-lacZ)U169 phoA glnV44 Φ80Δ (lacZ)M15 gyrA96 recA1 relA1 endA1 thi-1 hsdR17	Shigekawa, & Dower, 1988

Table 3.3. Composition of the media together with the species used for indicated between brackets. % are given as weight/volume (w/v).

Medium	Composition
YPD (yeast)	2% bacterial peptone, 2% glucose and 1% yeast extract
SC (yeast)	2% glucose, 0.5% $(NH_4)_2SO_4$, 0.17% YNB and 0.2% Drop-out
LB (bacteria)	1% tryptone, 1% NaCl and 0.5% yeast extract

Drop-out refers to a mix containing 2.0g of all the amino acids except for adenine, histidine, leucine, lysine, methionine, tryptophan and uracil which are used as selection markers. In our case, the auxotrophic markers used were leucine or histidine therefore, SC was complemented with all the amino acids listed previously, except for leucine or histidine depending on the experiment. The amino acid concentrations used were the following: 20µl/ml for adenine, uracil, histidine, tryptophan and methionine; while 30µl/ml for leucine and lysine.

In order to make plates from the media, agar was added up to 2% (w/v). In addition, ampicillin (Amp) and chloramphenicol (Chl) were added to LB medium to a final concentration of 75µg/ml and 25µg/ml, respectively, being the stock concentration 50 mg/ml and 25 mg/ml. For the LB

medium containing kanamycin (Kan) and chloramphenicol (Chl), the concentrations were 50µg/ml and 25µg/ml, respectively, with stock concentration of 50 mg/ml and 25 mg/ml.

Table 3.4. Plasmids used, main characteristics and origin or reference. The number indicated with a hash corresponds to the plasmid number in SRN collection.

Plasmid	Description/Application	Origin/ Reference
pRS315 (#21)	Yeast vector for new plasmids (LEU2 marker)	Sikorski and Hieter, 1989
pRS315-Mog1 (#559)	Expression of Mog1	Lu et al. 2004
pRS315-Mog1-E65K (#617)	Expression of Mog1E65K mutant	Oliete-Calvo et al. 2018
pRS315-Mog1-W145A (#618)	Expression of Mog1W145A mutant	Joan Serrano Quílez (SRN group)
pRS315-Mog1-E65K-W145A (#620)	Expression of Mog1E65KW145A mutant	Joan Serrano Quílez (SRN group)
pRS315-Mog1-K189A (#641)	Expression of MogK189A mutant	Joan Serrano Quílez (SRN group)
pRS315-Mog1-ΔK144-T153 (#645)	Expression of Mog1 mutant lacking the region from K144 to T153.	Joan Serrano Quílez (SRN group)
pRSII403-HIS3 (#48)	Obtainment of cassette for *MOG1* gene substitution by HIS marker	Chee and Haase, 2012
pET28b-HTB1 (#324)	Inducible overexpression of H2B tagged with N-terminal His6 tag (Kan marker)	Xuetong Shen's group
pGEX4T-1-Mog1-GST (#562)	Inducible overexpression of Mog1 tagged with N-terminal GST (Amp marker)	Lu et al. 2004
pET28b-HTB1 (#644)	Inducible overexpression of H2B tagged with N-terminal His6 tag (Kan marker).	This work: Stop codon removed from #324
pGEX4T-Mog178-218- GST (#561)	Inducible overexpression of a short version of Mog1 tagged with N-terminal GST (Amp marker)	Lu et al. 2004

Table 3.5 Primary antibody used for immunoblotting

Antibody	Host	Dilution	Origin/ company
α-His6	-	3:1000	Gift from Jeronimo Bravo's lab

Table 3.6. Primers used together with their sequence and application. The number indicated with a hash corresponds to the oligo number in SRN collection.

Primer	5'→3' sequence	Use
A3-HTB1 (#1602)	CACCCTGACACTGGTATTTC	Sequencing
A1-MOG1 FW (#1004)	GCGCTATTCTTGTTGTCTTC	PCR
A4-MOG1 RV (#1005)	GCTGTCTTCCGAGTAGAGTG	PCR
A4-pET28b (#1902)	TAGTTATTGCTCAGCGGTGG	Sequencing

A2-HTB1 FW (#1904)	TCTACTCAAGCACTCGAGCACCACCACCACCACCACTGAG	Quick-change
A3-HTB1 RV (#1903)	TGCTCGAGTGCTTGAGTAGAGGAAGAGTACTTGGTAACAG	Quick-change

3.2 Agarose gel electrophoresis

Nucleic acid gel electrophoresis was performed in a 1% (w/v) agarose gel using TAE buffer 1X (40mM Tris-acetate, 1mM EDTA pH 8.0). After adding the agarose, the mixture was heated in a microwave until it was completely dissolved. When cooled enough, green safe was added to a final concentration of 0.5µg /mL (10mg/mL stock solution). Then, the agarose gel was poured into a gel tray with a well comb in place and let solidify at room temperature. When the agarose was completely solidified, it was placed into the gel box.

Loading buffer 6X (0.25% (w/v) bromophenol blue, 0.25% (w/v) xylene cyanole blue, 30% (v/v) glycerol 50% (v/v), 12% (v/v) TAE 50X), was added to each of the DNA samples up to 1X before loading them into the wells. After loading all the samples and the molecular weight marker (100bp), the cuvette was filled with TAE 1X until covering the gel. Then, the gel was run horizontally at a constant voltage of 80V until the dye line was approximately at 80% of the bottom of the gel. Finally, the DNA fragments were visualised using a UV transilluminator (Ultima 16si-PLUs, Isogen®) and the images were analysed using the software Image Studio Lite (Li-COR Bioscience®).

3.3. Discontinuous polyacrylamide gel electrophoresis

Proteins were separated in denaturing 12 or 15% SDS-PAGE gels which consist of a separating and a stacking phase. The separating phase in case of 15% SDS-PAGE gel was prepared with 7.5mL of a solution of 30% (w/v) acrylamide 0.8% (w/v) bisacrylamide; 3.75mL Tris-HCl/SDS pH 8.8; 3.75mL MilliQ water to which 50 µL of 10% APS and 10µl of TEMED were added to allow the polymerization reaction. For 12% SDS-PAGE gel, the following volumes were used: 6ml of the acrylamide/polyacrylamide solution; 3.75ml Tris-HCl/SDS pH 8.8; 5.25mL MilliQ water; 50 µL of 10% APS and 10µl of TEMED. The stacking gel was prepared in both cases using 0.65 mL of the acrylamide/bisacrylamide solution; 1.25 mL of Tris-HCl/SDS pH 6.8; 3.05 mL MilliQ water; 25µL of 10% APS and 5µL of TEMED.

Before loading the samples, loading buffer 4X (50% (v/v) Tris 0.5M pH 6.8, 40% (v/v) glycerol 100% (v/v), 9.2% (w/v) SDS and 0.2% (w/v) bromophenol blue) was added to each sample up to 1X and heated to enhance denaturation and reduce the viscosity of the glycerol. Running buffer pH 8.3 consisted of 25 mM Tris-base, 190 mM glycine and 0.01% (w/v) SDS. The electrophoresis was performed in cuvettes at a constant voltage of 120V for a period enough for protein separation.

3.4. Plasmid recovery from DH5α electrocompetent *E. coli*

The collection of plasmids used were recovered from DH5α electrocompetent *E. coli* cells using the Wizard® Plus SV Minipreps DNA Purification System from Promega® according to the manufacturer protocol.

3.5. Transformation of yeast strains with plasmids

For an efficient transformation, the LiAc/SS carrier DNA/ PEG method designed by Gietz and Schiestl (2007) was used with the following modifications. Yeast cells were let grow in 50mL Falcon tubes containing 10mL of liquid YPD at 30ºC and 160rpm up to an OD_{600} value of 0.8-1.0. Then, cells were harvested by centrifugation at 3000 rpm (TX-150 rotor) for 5 min. After decanting the supernatant, the pellets were washed in 10mL of sterile MilliQ water and resuspended by vortexing. After that, a second centrifugation-resuspension step was performed but, in this case, resuspending the cells in 1mL of sterile MilliQ water. This mL was transferred

to a 1.5mL microcentrifuge tube and centrifuged for 30 sec at 13.000rpm, discarding the supernatant after. The pellets were then resuspended with 1mL of sterile MilliQ water and vortexed. 200µL of the cell suspension were transferred to new microcentrifuge tubes and centrifuged for 30sec at 13.000rpm. Then, 360µL of the transformation mix were added and resuspended using a pipette. 2µL of the appropriate plasmid (approximately 200ng) were added to the cell suspension and the tubes were incubated in a water bath at 42ºC with 650 rpm agitation for 40 min. Following incubation, the samples were centrifuged at 13.000 rpm for 30 seconds and the transformation mix removed with a pipette. The pellet was resuspended with 500µL of sterile MilliQ water and centrifuged again at 13.000 rpm for 30 seconds. The samples were finally resuspended in 100µL of sterile water, plated on selection medium and incubated at 30ºC for 2 or 3 days. All the centrifugation steps were performed at 4 ºC and those at 13.000 rpm, with F45-24-11 rotor.

The transformation mix was made of 240µL 50% (w/v) PEG, 36µL 1M LiAc, 50µL of carrier DNA (salmon sperm DNA, 2 µg/µL) and 34µL of sterile water per sample. The salmon sperm DNA must be boiled for 5 min and let chill on ice before being added to the mix.

3.6. Creation of the double mutant *set1Δmog1Δ*

3.6.1. Transformation of *set1Δ* yeast cells with cassette

The protocol designed by Gietz and Schiestl (2007) was used with the following modifications. *set1Δ* yeast cells were grown in 30mL of YPD liquid medium at 30ºC and 160 rpm up to an OD_{600} value of 0.5-0.8. Cells were harvested in 50mL Falcons and centrifuged at 3000 rpm (TX-150 rotor) for 3 min. Then, the supernatant was discarded, and the pellet washed with 10mL of cold sterile MilliQ water. After resuspension, the samples were centrifuged again at 3000 rpm (TX-150 rotor) for 3 min, discarding the supernatant and resuspending the pellet in 1mL of sterile MilliQ water. Then, the samples were transferred to microcentrifuge tubes and centrifuged at 3000 rpm (F45-24-11 rotor) for 3 min. The pellet was resuspended in 1mL of sterile MilliQ water and from this mL, 120µL were transferred to new microcentrifuge tubes and centrifuged as before. Once the supernatant was discarded, 350µL of the transformation mix and 2µL of cassette mog1::HIS3 (Table 3.4, Materials and Methods) were added. The transformation mix was made of 240µL 50% (w/v) PEG, 36µL 1M LiAc, 50µL of salmon sperm DNA (2µg/µL) and 34µL of 10X TE.

The cell suspension was incubated at 30ºC for 30 min and then, at 42ºC in a water bath for 20 min with agitation. After that, the samples were chilled on ice for 2 min and centrifuged at 3000 rpm (F45-24-11 rotor) for 2 min to remove the transformation mix. The pellet was resuspended in 5mL liquid YPD and incubated for 2h at 30ºC for recuperation. After incubation, samples were centrifuged as previously and resuspended in 1mL of sterile water. Finally, 100µL of *set1Δ* transformed cells were plated in SC-His solid medium and let grow for 2 or 3 days. All the centrifugation steps were performed at 4 ºC

3.6.2. Verification of Mog1 deletion

3.6.2.1. DNA extraction from yeast

Genomic DNA was extracted from *set1Δmog1Δ* cells according to the protocol described by Blount et al. (2016). *set1Δmog1Δ* colonies were inoculated into 50ml Falcon containing 10ml YPD and let grow overnight at 30ºC and 160 rpm. Cells were harvested and centrifuged at 13000 rpm (F45-24-11 rotor) for 1 min and the growth medium discarded. Then, the pellet was washed with MilliQ water and resuspended in 100µL 5% (v/v) Chelex 100 resin. Glass beads were added to half total sample volume and vortexed at high speed and 4ºC for 4 min (1 min on/ 1 min off). After that, the samples were incubated at 100ºC for 2 min followed by centrifugation at top speed for 1 min. The supernatant was collected and transferred to a new microcentrifuge tube without

taking the beads and Chelex. Finally, the extracted MilliQ was quantity and quality checked by Nanodrop. All the centrifugation steps were performed at 4ºC.

3.6.2.2. PCR

The polymerase chain reaction (PCR) was performed using primers annealing to the flanking region of the *MOG1* gene (Table 3.6). 20µL of the PCR mix was prepared per sample containing 1µL Taq Polymerase Buffer 10x (Roche®) including $MgCl_2$; 2µL 4 mM dNTPs (Invitrogen®); 1µL 10µM reverse primer; 1µL 10µM forward primer; 0.2µL Taq Polymerase (Roche®); 1µL DNA template (approximately, 100 ng genomic DNA/20µl PCR mix) and 11.8µL MilliQ water.

The PCR programme for cassette amplification consisted of an initial denaturation step of 3 min at 95ºC; 9 cycles of 15 sec at 95ºC followed by 30 sec at 54ºC and 2 min at 72ºC which corresponded to the first denaturation, annealing and amplification; 25 cycles of 15 sec at 95ºC with 30 sec at 54ºC and 2 min + 5 sec/cycle at 72 ºC for more cycles of denaturation, annealing and amplification; final extension at 72ºC for 7 min and a final holding temperature of 4ºC. The PCR products were analysed by agarose gel electrophoresis according to the protocol described in Materials and Methods 3.2.

3.6.3 Storage of the strain

The new strain was glycerinated to be kept in the collection at -80ºC. For that, one colony was inoculated into 50ml Falcon tubes containing 5ml of YPD and let grow at 30ºC and 160rpm until an OD_{600} of 0.6-0.8. 600µL of the cell culture were transferred to a sterile 2ml microtube with screwcap. Then, 400µL of sterile 50% (v/v) glycerol were also added and the tubes rapidly frozen with N_2 liquid to avoid toxicity due to glycerol.

3.7. Growth assay

Transformed yeast cells were grown in 5ml SC-Leu liquid medium o/n. Saturated overnight cultures were diluted into fresh media to an OD_{600} value of 0.3 and let duplicate (≈2-3h). At this point, they were diluted again to OD_{600} values of 0.1-0.2, equalising the OD_{600} values amongst the different samples. Five serial dilutions (1; 1:10; 1:100; 1:1000; 1:10000, 1:100000) were prepared for each strain in a 96-well plate. 8µL drops were placed in SC-Leu plates in rows and columns, being the five dilutions of the same strain in a row. Two plates were prepared with the same samples and incubated one at 30ºC and the other one at 37ºC for 24-72h. Two biological replicates for each condition were prepared.

3.8. Growth curves

Yeast cell cultures were prepared as in Materials and Methods 3.7. In this case, three biological replicates were used for each strain. Instead of preparing serial dilutions, 260µL of each cell culture were plated in a 96-well plate (VWR® Tissue Culture Plates). Three wells were filled with 260µL of medium as the blank. The OD_{600} was measured each 20min with continuous shaking between readings during 22h at 30 ºC or 37 ºC in a multimode microplate reader (Spar®, TECAN).

3.9. IPTG induced protein expression in BL21-CodonPlus (DE3) *E. coli*

3.9.1. Preparing BL21-CodonPlus (DE3) *E. coli* competent cells

BL21-CodonPlus (DE3) *E. coli* cells were plated on LB plates containing 25µg/ml chloramphenicol and incubated at 37ºC overnight. One colony was inoculated in 10mL of LB (+ chloramphenicol) liquid medium and let grow overnight at 37ºC and 250 rpm. From these 10 mL, 2mL were saved for blank and 5mL of the culture were transferred into 500mL LB (+ chloramphenicol) in 2L flasks and allowed to grow at 37ºC and 250 rpm until OD_{600} ≈0.4. Then, the cells were transferred to 2 centrifuge bottles (250mL) and placed on ice for 20 min. After that, cells were centrifuged at 3000rpm (Sorval RT6000B rotor) for 10 min and resuspended in 30mL

of cold 0.1M $CaCl_2$. The cell suspension was transferred to 50mL Falcon tubes and incubated on ice for 30 min. After incubation, cells were centrifuged at 3000rpm (Sorval RT6000B rotor) for 10 min, the supernatant was discarded, and the pellet was resuspended by pipetting 8mL cold 0.1M $CaCl_2$ containing 15% (v/v) glycerol. Finally, 140µL aliquots of the cell suspension were transferred to 1.5mL microcentrifuge tubes and placed on ice for transformation or frozen at -80 ºC until use. All the centrifugation steps were performed at 4ºC. Protocol from Chang et al. (2017).

3.9.2. Transformation of BL21-CodonPlus (DE3) *E. coli*

BL21-CodonPlus (DE3) competent *E. coli* cells were transformed following the protocol developed by Chang et al. (2017). 1µL of the correspondent DNA plasmid (approximately 100ng) was added to BL21-CodonPlus (DE3) competent *E. coli* cells and mixed by inversion for 4-5 times. Then, the tubes were placed on ice for 30 min for maximum transformation efficiency, followed by incubation in a water bath at 42ºC for 45 sec while shaking. After that, the tubes were placed on ice for 2 min and recovered by adding 1mL of LB to each of the tubes, incubating at 37ºC and 60 min while shaking. Finally, the cell samples were centrifuged at 3000 rpm (F45-24-11 rotor) for 3 min and 4ºC and resuspended in 100µL of sterile MilliQ water. Then, they were placed onto a LB selection plate containing chloramphenicol (25µg/ml) and kanamycin (50µg/ml) or ampicillin (75µg/ml) and incubated overnight at 37ºC.

3.9.3. IPTG induced protein expression test

One colony of BL21-CodonPlus (DE3) competent *E. coli* cells transformed with the desired expression plasmid was inoculated into 50mL Falcon tubes containing 10mL LB medium (+chloramphenicol and kanamycin/ ampicillin) per sample and let grow at 37ºC and 200rpm until an OD_{600} of 0.6-0.8. Before adding IPTG (1M stock concentration), 1 mL of each sample was collected as the -IPTG sample for checking the basal expression of the protein. Then, IPTG was added to a final concentration of 1mM and the samples were incubated at 16ºC and 200rpm o/n. After the incubation period, two samples of 1mL were taken as +IPTG and soluble/insoluble fraction samples.

The microcentrifuge tubes containing the three samples were centrifuged for 1 min at 4ºC and 13000rpm (F45-24-11 rotor). The resulting pellet was introduced in liquid nitrogen until completely freezing and then, 200µL of lysis buffer added to each sample. After this, cell disruption was performed by sonication on ice with an amplitude of 50% with pulses of 30 sec followed by 30 sec pauses for 10 min/sample using SoniPrep 150 (Sanyo®). In case of the fraction samples, after sonication the soluble and insoluble fractions were separated by centrifugation for 10min at 4ºC and 5500 rpm (F45-24-11 rotor). Finally, loading buffer 4X was added to each sample up to 1X to run a polyacrylamide gel according to the procedure described in Materials and Methods 3.3. The gel was stained with Blue Safe® during 20 min to observe the protein bands. Two lysis buffers were used depending on the protein to be purified: lysis buffer A (50mM Tris-HCl pH 8, 5M NaCl and 20mM imidazole) and lysis buffer B (PBS 1X pH 7.3). PBS 10X is made of 0.02% (w/v) KCl, 0.02% (w/v) KH2PO4, 0.12% Na2HPO4 and 0.8% (w/v) NaCl. This protocol was adapted from Ivić et al. (2016).

3.9.4. Scale up

1L of BL21-CodonPlus (DE3) competent *E. coli* cells transformed with the desired expression plasmid were grown to obtain enough protein content. For this, one colony was inoculated in 50mL Falcon tubes containing 5mL of LB plus chloramphenicol and kanamycin/ampicillin and let grow overnight at 37ºC and 200 rpm. 1ml of the cell culture was added to 500ml of fresh medium (+selection markers) in 2L flasks, preparing two flasks, and incubated at 37ºC and 200 rpm until OD_{600} was 0.6-1.0. Then 1mL was taken, centrifuged at 13000 rpm (F45-24-11 rotor) for 1 min and frozen with N_2 liquid as the -IPTG sample. Then, 1mM IPTG was added to the cell culture followed by incubation at 16ºC and 200 rpm o/n. After incubation, 2ml were taken as the

-IPTG and the fraction samples and processed as in the expression test (Materials and Methods, 3.9.3). Then, the cultures were collected in 500ml centrifuge tubes and centrifuged at 4000 rpm (SLA-3000 rotor) and 4ºC for 30 min. The supernatant was removed, and the pellet resuspended in 30mL of the correspondent lysis buffer. The cell suspension was transferred to 50mL Falcon tubes and finally centrifuged at 4000 rpm (TX-150 rotor) and 4ºC for 20 min and the pellet frozen with N_2 liquid and stored at -80ºC until use. This protocol was adapted from Ivić et al. (2016).

3.10. Protein purification

3.10.1. His-tagged H2B. Immobilized Metal Affinity Chromatography (IMAC)

For the purification of the His-tagged H2B, affinity column purification was performed adding TALON® Superflow ™ resin (GE Healthcare Life Sciences®) to a column (Bio-Rad®). First, the cell pellet kept on -80ºC was resuspended in 25mL of washing buffer A (same as lysis buffer A, Materials and Methods, 3.9.3) and transferred into a beaker set on ice. Then, the cells were lysed by sonication with an amplitude of 50% with pulses of 30 sec followed by 30 sec pauses for 30 min/sample using SoniPrep 150 (Sanyo ®). After sonication, 20µL were collected and called "TOTAL" sample, transferring the rest of the cell suspension into 500mL centrifuge tubes for centrifugation at 18000rpm (SS34 rotor) and 4ºC for 30 min. Additionally, a 20µL aliquot was taken from the supernatant and named "SOLUBLE". sample. The supernatant was collected and transferred to a new Falcon tube for purification. This soluble fraction was filtered with 0.45µm filter to avoid accumulation of aggregated or precipitated proteins. The pellet was resuspended with washing buffer A, taking a 20µL aliquot as the "INSOLUBLE" sample.

Before adding the soluble fraction to the column, the column was equilibrated. For this, 1mL of washing buffer A was poured into the column and let flow through the column. Then, 1mL of TALON beads were pipetted into the column and let drain without letting the beads to completely dry. Finally, the beads were washed by adding 5CV of washing buffer (5 times the volume occupied by the beads in the column) and let to drain.

After column equilibration, the filtered soluble fraction was poured into the column collecting the flow through and taking a 20µL aliquot as the "FLOWTHROUGH" sample. Then, the column was washed 3 times with 5CV of washing buffer A taking 20µL from each washing step for "WASH 1, 2, and 3" samples. After that, protein elution was performed by adding 0.5CV of elution buffer A (50mM Tris-HCl pH 8, 5M NaCl and 250mM imidazole) six times and taking a 10µL aliquot for each elution step as "ELUATE 1, 2, 3, 4, 5, 6" samples. Then, the column was washed with 2CV of elution buffer A, followed by 5CV of MilliQ water and 5CV of 20% (v/v) ethanol. All the steps during cell lysis and purification were performed at 4ºC. This protocol was adapted from Bornhorst and Falke (2000).

Later, all the samples taken during the procedure were run in a polyacrylamide gel (Materials and Methods, 3.3) and the gel stained with Blue Safe ® during 20 min to check the efficiency of the purification.

Finally, the eluates containing the most intense bands were combined and dialysed using a dialysing tube (Membra-Gel ®, SERVA) which was introduced into a 2L beaker containing 2L of washing buffer A to reduce imidazole content from the protein solution. The final protein content was quantified by Bradford assay. Then, the protein containing samples were aliquoted and frozen in N_2 liquid rapidly to be stored at -80ºC until use.

3.10.2. GST-Tagged Mog1 and GST-tagged Mog1 78-218. Glutathione Sepharose Chromatography.

GST-tagged Mog1 and GST-tagged Mog1 78-218 proteins were purified by affinity chromatography following the same procedure as with H2B but changing both the beads and the buffers used. In this case, glutathione sepharose beads were used (GE Healthcare ®) instead. The lysis and washing buffers consisted on PBS 1X pH 7.3 (lysis buffer B) while the eluting buffer B contained 50mM Tris-HCl pH 8 and 10mM reduced glutathione pH 8.0. This protocol was adapted from Harper and Speicher (2011).

3.11. Sequencing

For sequencing, 10µL of the plasmid to be sequenced (≈100ng) and 10µM of the correspondent primer were sent in separate microcentrifuge tubes to the sequencing service.

3.12. Site-directed mutagenesis

3.12.1. Quick-change

To delete the stop codon (TAA) of the *HTB1*-His tagged gene in pET28b-*HTB1*, a pair of overlapping oligos were designed annealing to both sides of the stop codon but lacking it (Table 3.6). PCR mix was prepared by adding 10ng of the pET28b-*HTB1*; 0.5µL Phusion Taq polymerase® (ThermoFisher™); 10µL Taq polymerase buffer 5X; 2.5µL dNTPs 4mM; 2.5µL FW primer; 2.5µL RV primer and MilliQ water up to 50µL per sample. PCR was performed in a thermocycler applying the following parameters: 30s at 98ºC for the initial denaturation, 35 cycles of 10s at 98ºC, 30s at 62ºC and 2 min at 72ºC for denaturation, annealing and amplification; a final extension for 5min at 72ºC and final holding at 4ºC. The protocol was designed following the recommendations from Phusion™ Site-directed Mutagenesis Kit user guide (THERMOSCIENTIFIC, 2019).

Three different conditions were tested: (1) using HF Phusion buffer® as the Taq polymerase buffer, (2) using HF Phusion buffer® and adding 5% DMSO to the transformation mix, (3) using GC Phusion buffer® as the Taq polymerase buffer. For each of the conditions, three samples were prepared: one lacking the plasmid (PCR negative control), one lacking the Taq polymerase (mutagenesis negative control) and one containing all the components.

3.12.2. Verification of stop codon deletion

After PCR, the nine samples were run in a 1% agarose gel using a 1kB marker. For that, to 2µL of each sample, 3µL MilliQ water and 1µL loading buffer 6X were added and loaded into the wells (Materials and Methods, 3.2.).

3.12.3. DpnI treatment

Following Quick-change Site Directed Mutagenesis Kit Instruction Manual (AGILENT TECHNOLOGIES, 2015b), 1µL DpnI was added to the three samples and to those being the negative control for mutagenesis and incubated for 3h at 37ºC in a thermocycler.

3.12.4. Plasmid recovery

DH5α competent *E. coli* cells (Invitrogen®) were transformed with the six samples treated with DpnI. For that, the High Efficiency Transformation Protocol (NEW ENGLAND BIOLABS, 2019a) was followed. 3µL of the positive samples were added to 50µL of cell aliquot and kept in ice for 30 min. After that, they were subjected to a heat shock in a water bath for 45 sec at 42ºC and then chilled on ice for 5 min. Recuperation was performed by adding 450µL SOC medium (Invitrogen®) per sample and incubating at 37ºC for 1h. After transformation, cells were plated on LB medium containing 50µg/ml kanamycin and incubated overnight at 37ºC. Then, one colony was inoculated into 5ml of LB medium (+kanamycin) and let grow at 37ºC and 250rpm until

OD_{600} 0.6-0.8. Finally, the plasmid was recovered following the same procedure as in section 3.4.(Materials and Methods) and sent for sequencing (Materials and Methods, 3.12).

3.12.5. Transfer and immunoblotting

BL21-CodonPlus (DE3) *E. coli* cells were transformed with the new plasmid pET28b-*HTB1* and the expression of the His tagged H2B protein was induced and analysed following the same procedure as in Materials and Methods 3.9.2-3.9.3. Once the proteins were separated by electrophoresis, they were transferred to a 0.45µm nitrocellulose membrane (Amersham Protran, GE Healthcare Biosciences®) and covered by wipers (Wipall, Kimberly-Clark ®) on both sides for semi-dry transfer. The buffer used was Bjerrum and Schafer-Nielsen buffer (48mM Tris, 39mM glycine, 20% Methanol (v/v), pH 9.2) kept at 4ºC. The transfer was performed in Trans-Blot Turbo Transfer System ™ (Bio-Rad®) applying an optimised protocol for 1.5mm Mini gels using a voltage of 25V for 10 min.

After that, the proteins were stained with a solution of Ponceau 1% (w/v) in 1% (v/v) acetic acid for 1-2 min and washed with distilled water. Then, the membrane was blocked with 10mL of a solution containing 5% (w/v) milk powder with TBS-Tween (0.02M Tris-HCl pH 7.6 and 0.8 % (w/v) NaCl-0.01% (v/v) Tween-20) for an hour at room temperature while shaking. Following blocking, the membrane was incubated for 1 hour with an antibody binding the histidine tail (Table 3.5, Materials and Methods) diluted in TBS-Tween with 5% (w/v) powder milk. Then, three washing steps were performed with TBS-Tween for 5-10 min while shaking. During incubation and washing, the membrane was covered by aluminium foil. The membrane was revealed in a luminescent image analyser ImageQuant LAS 4000 mini (GE Healthcare ®).

3.12.6. Storage of the plasmid

To store the plasmid in the collection, DH5α electrocompetent *E. coli* cells (New England BioLabs®) were transformed by electroporation with the plasmid, glycerinated and stored at -80ºC following the Electroporation Protocol (NEW ENGLANDS BIOLABS, 2019b). For that, electroporation cuvettes were first sterilized with UV light using Stratalinker ® UV Crosslinker 1800 for 5min and let chill on ice. Meanwhile microtubes containing 50µL of DH5α *E. coli* electrocompetent cells were prepared, one for each transformation plus one negative control, and let chill on ice too. 1µL of the plasmid (≈ 100ng) was added to the cell suspension and then the cell/DNA mix transferred to a chilled electroporation cuvette maintaining sterile conditions and without introducing bubbles. Electroporation was performed with Eppendorf Electroporator 2510 using the following conditions: 1.7kV, 200 Omega and 25µF. The time constant was 4.8 to 5.1 milliseconds which corresponded to two rapid pulses. Immediately after, 450µL of LB were added to the cuvettes and the cell suspension transferred to a microcentrifuge tube for incubation at 37ºC and 750rpm for 40-60 min. After recuperation, tubes were centrifuged at 3000rpm (F45-24-11 rotor) and 3 min at room temperature and the supernatant discarded. The cell pellet was finally resuspended in 100µL of sterile MilliQ water, plated on LB +Kanamycin and incubated at 37ºC for 24h.

One colony of each of the transformants was inoculated into 5ml LB plus 50µg/ml kanamycin and grown at 37ºC and 250rpm until OD_{600} 0.6-0.8. To glycerinate the cell culture, the procedure was the same as in section 3.6.3 but 700µL of the cell culture and 300µL of glycerol were used instead.

3.13. Pull down assay

Approximately 100µL of beads with affinity to the tag of the protein used as the bait, were poured into a 1.5mL microcentrifuge tube, washed with 1mL MilliQ water and the supernatant removed after centrifugation. The beads were washed again with a washing buffer, A or B depending on the protein used as the bait, and centrifuged without completely removing the supernatant. 100-

200µg of the purified tagged protein were incubated with the beads for 30min at 4ºC and constant rotation. After incubation, the sample was centrifuged, and the supernatant was collected as "FLOWTRHOUGH" sample. The beads were washed with 1mL of washing buffer, centrifuged and the supernatant collected as "WASH" sample. The washing step was repeated twice.

Then, the second purified protein, the pray, was added to the beads in equimolar concentration to the bait protein and incubated for 30min at 4ºC and constant rotation. The sample was centrifuged and collected as "FLOWTHROUGH 2" sample. The beads were then washed with 1mL of the same washing buffer as before and re-centrifuged to collect the supernatant as "WASH" sample. This step was repeated twice. Finally, the beads were collected adding 30µL of loading buffer 4X and boiling for 10min to obtain the "ELUTION" sample. From all the samples collected during the different steps of the procedure, 20µL were taken and loading buffer 4X was added up to 1X. Then, the samples were run in a polyacrylamide gel electrophoresis (Materials and Methods, 3.3) and dyed with Blue Safe® for 20min. Centrifugation was done in all the steps at 5000rpm (F45-24-11 rotor) and 4ºC for 5min.

In parallel to this assay, another pull-down was performed adding only the pray protein at the same concentration as in the previous one to test unspecific binding to the beads.

4. RESULTS

4.1. Creation of the double mutant *set1Δmog1Δ* from *set1Δ* strain

Three clones of *set1Δ S. cerevisiae* cells were transformed with the previously PCR-constructed cassette from pRSII403-*HIS3* (Table 3.4, Materials and Methods) for the deletion of the *MOG1* gene, and grown in SC-His for the selection of the transformants as explained in Materials and Methods, 3.6.1. The substitution of the *MOG1* gene by the selection marker *HIS3* is performed by homologous recombination because the *HIS3* gene in the cassette is flanked by homologous regions to those flanking the *MOG1* gene in the genomic DNA. When the double-stranded PCR product is transformed into yeast, the genomic *MOG1* gene is replaced through a double cross over event (Appendix, Figure 8.1).

After transformation, DNA was extracted from the three clones (Materials and Methods, 3.6.2.1) and it was checked by PCR if the *MOG1* gene was correctly substituted by *HIS3* gene as expected. For that, 20nt oligos were designed annealing to the flanking regions of the *MOG1* gene and named A1-*MOG1* FW and A4-*MOG1* RV (Table 3.6, Materials and Methods). If *MOG1* gene (654bp) is substituted by *HIS3* (1184bp), a difference in the amplification product from the PCR experiment can be detected as a slower migrating band when running an agarose gel electrophoresis (Appendix, Figure 8.2).

Two out of the three clones bore *MOG1* deletion (Clones I and II), since the band size corresponded to the one expected for *HIS3* amplification. The third clone was invalid since the PCR failed, and no PCR product could be detected (Appendix, Figure 8.3).

4.2. Phenotypic effect of Mog1W145A and Mog1E65KW145A mutations in *mog1Δ* and *set1Δmog1Δ S. cerevisiae* growth

S. cerevisiae mutant strains *mog1Δ* and *set1Δmog1Δ* were transformed with pRS315 containing different versions of the Mog1 protein (Table 3.4, Materials and Methods): wild-type Mog1, Mog1 with a single point mutation in its residue 65 (glutamic acid (E) substituted by lysine (K)), Mog1 with a single point mutation in 145 (tryptophan (W) substituted by alanine (A)) and a Mog1 mutant containing both single mutations E65K and W145A (Materials and Methods, 3.5). The *set1Δmog1Δ* strain is deficient in H3K4 methylation and other cellular processes allowing the detection of more subtle differences in growth caused by Mog1 mutants. The growth of the *mog1Δ* and *set1Δmog1Δ* mutants was compared to the strain transformed with the empty plasmid (pRS315 without *MOG1*) and to the wild type strain (BY4741 for *mog1Δ* and *set1Δ* for *set1Δmog1Δ*) by growth assay on SC-Leu plates (Figure 4.1) as detailed in Materials and Methods, 3.7.

A slower growth phenotype is observed in *mog1Δ*+pEmpty strain compared to the WT both at 30ºC and 37ºC. This growth reduction is partially rescued when the Mog1 protein is expressed in a plasmid at 30ºC. Notably, Mog1 complementation is not complete at 37ºC. Both single point mutations E65K and W145A and the double mutation E65KW145A on *MOG1* cause a slower growth phenotype compared to the WT but not compared to *mog1Δ*+pMog1 at 30ºC. Since *mog1Δ*+pMog1 shows the phenotype caused by the wild type protein when expressed from a plasmid, it will be used as the reference strain to compare the phenotypic effect of *MOG1* mutations instead of the WT strain. At 37ºC the phenotype caused by the mutants is very different, growing better than *mog1Δ*+pMog1(Figure 4.1.A).

The absence of *MOG1* leads to a synthetic sickness phenotype when combined with a deletion of *SET1* both at 30ºC and 37ºC. Growth is partially recovered by the expression of *MOG1* in a plasmid when compared to *set1Δ* +pEmpty at both conditions. E65K and W145A single mutations and E65KW145A double mutation cause a slower growth phenotype at 30ºC compared to the *set1Δ* pEmpty strain but not to *set1Δmog1Δ*+pMog1 as seen in *mog1Δ*. However, at 37ºC both single mutations cause a reduction in growth compared to *set1Δmog1Δ*+pMog1, being this effect

stronger in the case of W145A, which shows a synthetically sick phenotype. The double mutant shows the same positive effect on growth as in the *mog1Δ* strain at 37ºC, in this case recovering the growth levels of the compensated phenotype. Therefore, in the *set1Δmog1Δ* strain there are significant phenotypic differences between the double mutant and the single mutants at 37ºC (Figure 4.1.B).

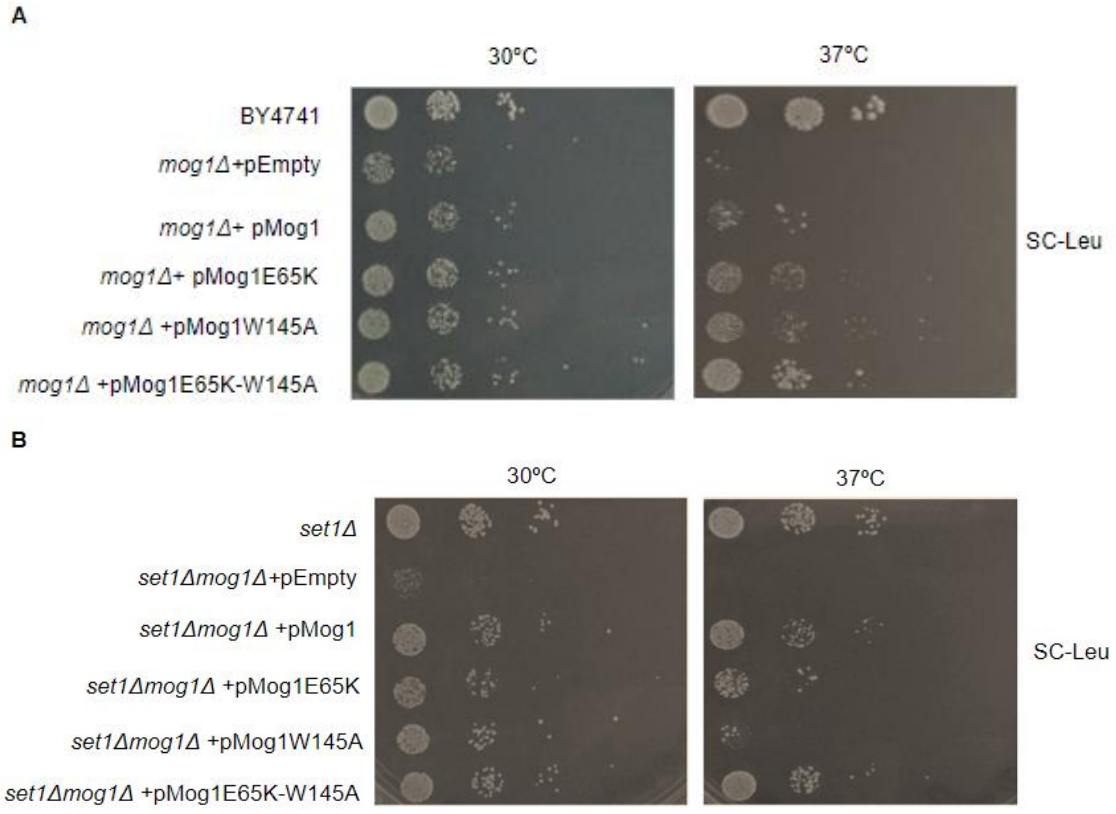

Figure 4.1. Growth assay of mog1Δ and set1Δmog1Δ strains carrying plasmids with different mutations on MOG1*. Ten-fold serial dilutions of the indicated strains were plated on SC-Leu and incubated at 30/37ºC for 2-3 days. Pictures were taken at 48h.*

4.3. Phenotypic effect of Mog1ΔK144-T153 and Mog1K189A mutations in *mog1Δ* and *set1Δmog1Δ S. cerevisiae* growth

S. cerevisiae mutant strains *mog1Δ* and *set1Δmog1Δ* were transformed with pRS315 containing different versions of the Mog1 protein (Table 3.4, Materials and Methods): wild-type Mog1, Mog1 with a single point mutation in 189 (lysine (K) substituted by alanine (A)) and Mog1 lacking the region from K144 to T153 which corresponds to part of the putative Shg1-Mog1 binding domain (Materials and Methods, 3.5). As in the previous section, *mog1Δ* and *set1Δmog1Δ* transformed with the empty plasmid pRS315, BY4741 and *set1Δ* strains were used to compare the effects caused by the mutations. In this case the growth was analysed by measuring the OD_{600} of the different cell cultures for 22h at 30ºC and 37ºC, except for *set1Δmog1Δ* at 37ºC which was recorded for 18h (Materials and Methods, 3.8). Growth curves were represented with the values obtained, normalising each data point to the OD_{600} of the blank (SC-Leu) at that point (Appendix, Figures 8.4 and 8.5). Since three biological replicates were used for each strain at both conditions, the average of the three values at each time point was calculated and represented together with error bars as the standard deviation (Figures 4.2 and 4.3).

Comparing WT (BY4741) and *mog1Δ* strains growth curves (Figure 4.2), the faster growth corresponds to the WT while the slowest to *mog1Δ*+pEmpty both at 30ºC and 37ºC, as expected.

When the Mog1 protein is expressed from a plasmid, the phenotype of the *mog1Δ*+pEmpty is not completely compensated in either condition since growth does not fully recovers WT levels as seen in WT/ *mog1Δ* growth assay (Figure 4.1). In this case, the growth curve of *mog1Δ*+pMog1 will be also used to compare those of the mutants since *mog1Δ*+pMog1 indeed represents the phenotype of Mog1 expressed from a plasmid. When analysing the mutants, both *mog1Δ*+pMog1K189A and *mog1Δ*+pMog1ΔK144-T153 seem to have the same phenotypic effect as *mog1Δ*+pMog1 at both temperartures, although growth is slightly higher in *mog1Δ*+pMog1.All the strains reached a higher OD_{600} at the stationary phase at 30ºC than at 37ºC although standard deviation is higher in the case of the mutants at 37ºC than at 30ºC.

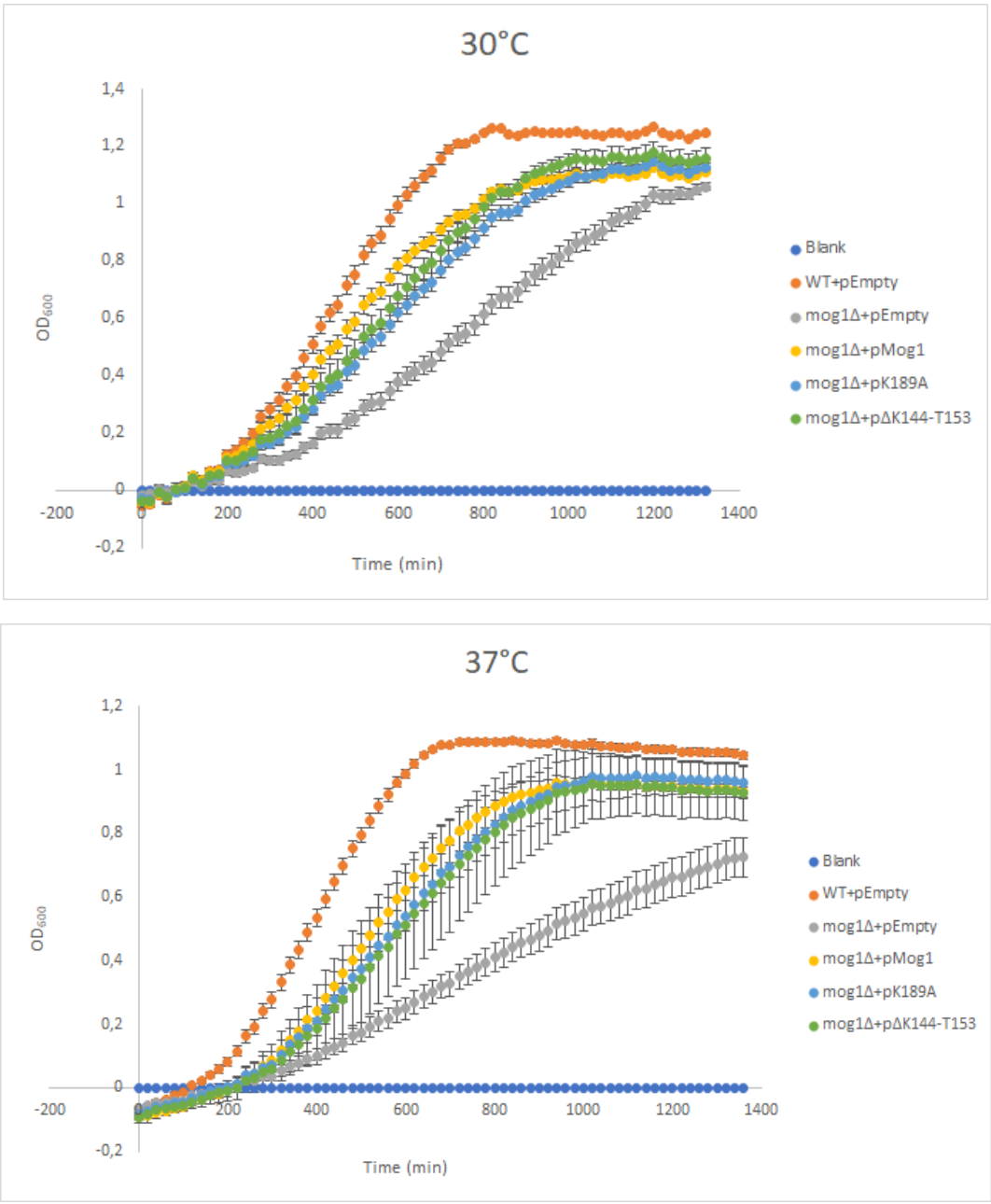

Figure 4.2. Growth curves of WT (BY4741) and mog1Δ strains. *OD_{600} values are represented over time (min) as the average of the three biological replicates for each strain with the corresponding standard deviation.*

When comparing *set1Δ* and *set1Δmog1Δ* (Figure 4.3), *set1Δmog1Δ*+pEmpty is the strain having the slowest growth at 30ºC showing a synthetically sick phenotype at 37ºC. When *set1Δmog1Δ*

is complemented with the wild type Mog1, growth is partially recovered without reaching growth levels of *set1Δ* in either condition as seen by *set1Δ/ set1Δmog1Δ* growth assay (Figure 4.1). In this case, there are differences compared to the phenotypic effect of the mutants in *mog1Δ*. In *set1Δmog1Δ*, *set1Δmog1Δ*+pK189A and *set1Δmog1Δ* +pΔK144-T153 grow better than *set1Δmog1Δ*+pMog1 showing almost the same behaviour as *set1Δ*+pEmpty at both temperatures. There is no significant difference with respect to the OD_{600} reached at the stationary phase between both temperatures.

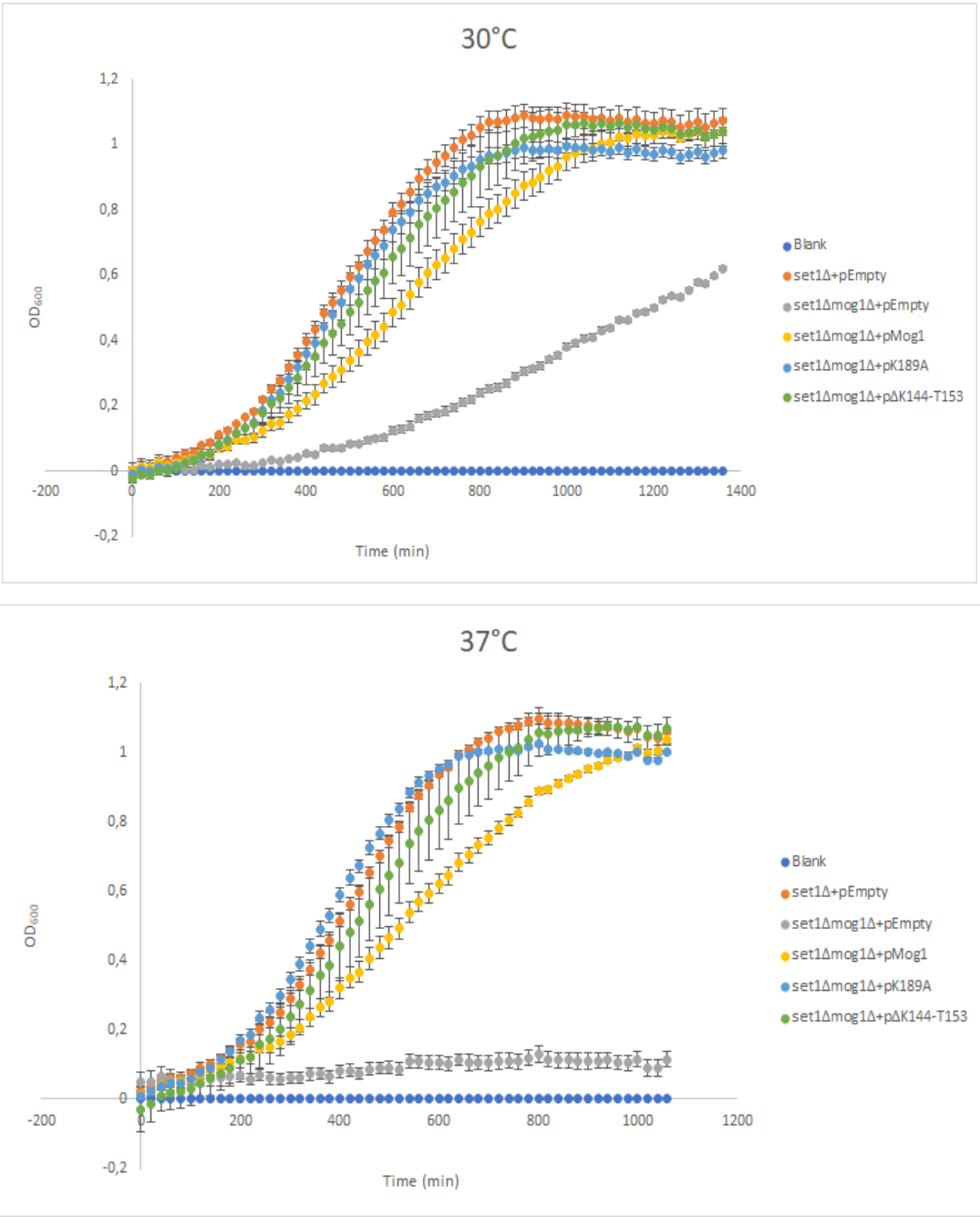

Figure 4.3. Growth curves of set1Δ and set1Δmog1Δ strains. *OD_{600} values are represented over time (min) as the average of the three biological replicates for each strain with the corresponding standard deviation.*

The phenotypic effects showed by the growth curves coincide with the growth rate and doubling time calculated for each of the strains (Appendix, Table 8.1). Growth rates were estimated from

growth curve data by taking the log of the exponential phase and performing linear regression according to the following equation:

$$A = A_o \cdot e^{\mu(t-t_o)} \longrightarrow lnA = lnA_o + \mu(t\text{-}t_0)$$

Where μ is the growth rate (min^{-1}), A is the absorbance at 600nm and t is time (min).

Doubling time is calculated from the previous equation by applying the definition of doubling time: $t_{\frac{1}{2}} \longrightarrow A = 2A_o$

$$ln\frac{A}{A_o} = \mu \cdot (t - t_o) \longrightarrow ln\frac{2A_o}{A_o} = \mu \cdot t_{\frac{1}{2}} \longrightarrow t_{1/2} = \frac{ln2}{\mu}$$

The estimated growth rate values were analysed for significant difference for each set of strains and temperature condition using ANOVA test and then, compared in pairs to the correspondent +pMog1 strain by t-test (Figure 4.4).

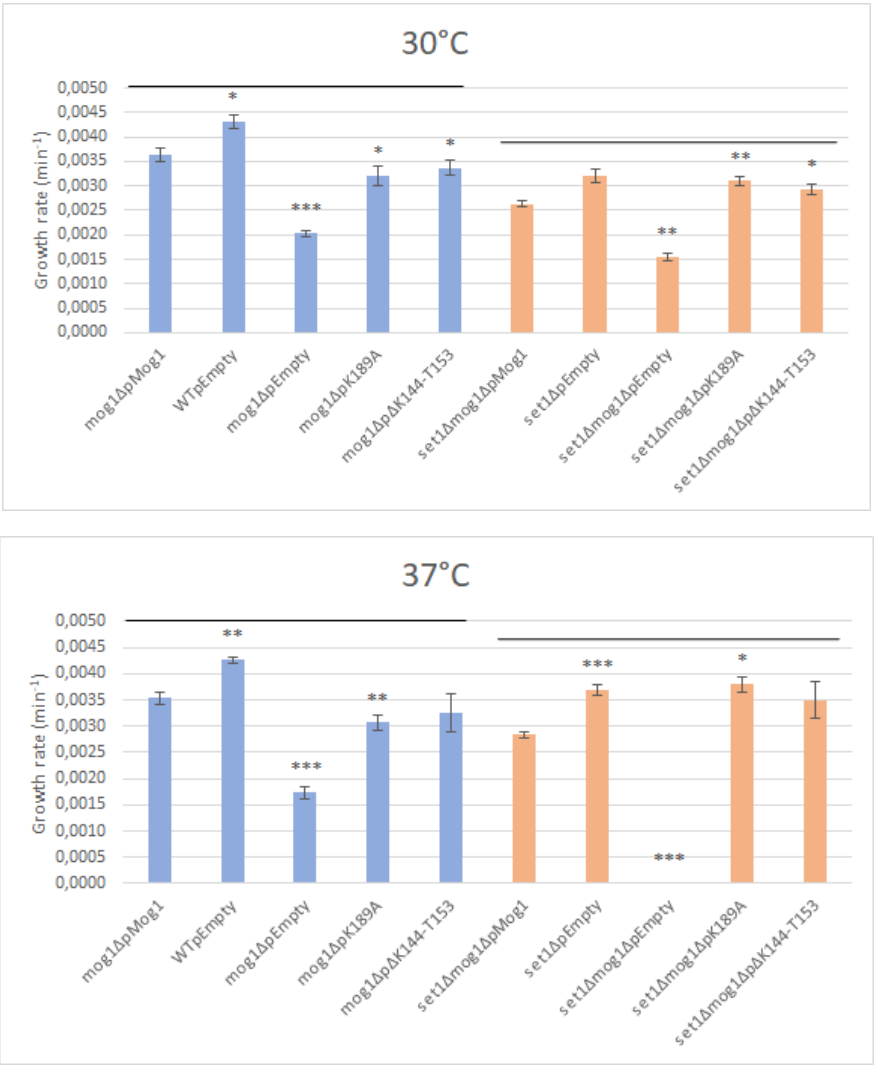

Figure 4.4. Growth rate values estimated for each of the strains and conditions. *The lines above the bars indicate the strains included in each ANOVA analysis which were then compared to the strain containing +pMog1 for significance. Those strains showing no significant difference correspond to those having only two replicates for the analysis (Appendix, Figures 8.4 and 8.5) (*) p<0.05; (**) p<0.01; (***) p<0.001.*

When comparing the growth rates between *mog1Δ* mutants and WT (Figure 4.4), the highest growth rate corresponds to the WT both at 30ºC and 37ºC. The lowest growth rate is shown by *mog1Δ* +pEmpty, being lower at 37ºC. Growth rate of *mog1Δ* +pMog1 is significantly lower than that of the WT but slightly higher than those of *mog1Δ* +pK189A and *mog1Δ* +pΔK144-T153 at both temperatures.

When comparing *set1Δ* and *set1Δmog1Δ* strains (Figure 4.4), growth rates are higher at 37ºC than at 30ºC in all the strains except for *set1Δmog1Δ*+pEmpty which shows a synthetically sick phenotype at 37ºC. As in *mog1Δ*strain, *set1Δmog1Δ*+pMog1 growth rate is significantly lower than that of *set1Δ*+pEmpty at both temperatures. However, the growth rates of *set1Δmog1Δ*+pK189A and *set1Δmog1Δ*+ pΔK144-T153 are significantly higher than that of *set1Δmog1Δ*+pMog1 both at 30ºC and 37ºC while they show no significant difference with *set1Δ*+pEmpty growth rates at any temperature (Appendix, Figure 8.6).

4.4. Protein-protein interaction assay workflow

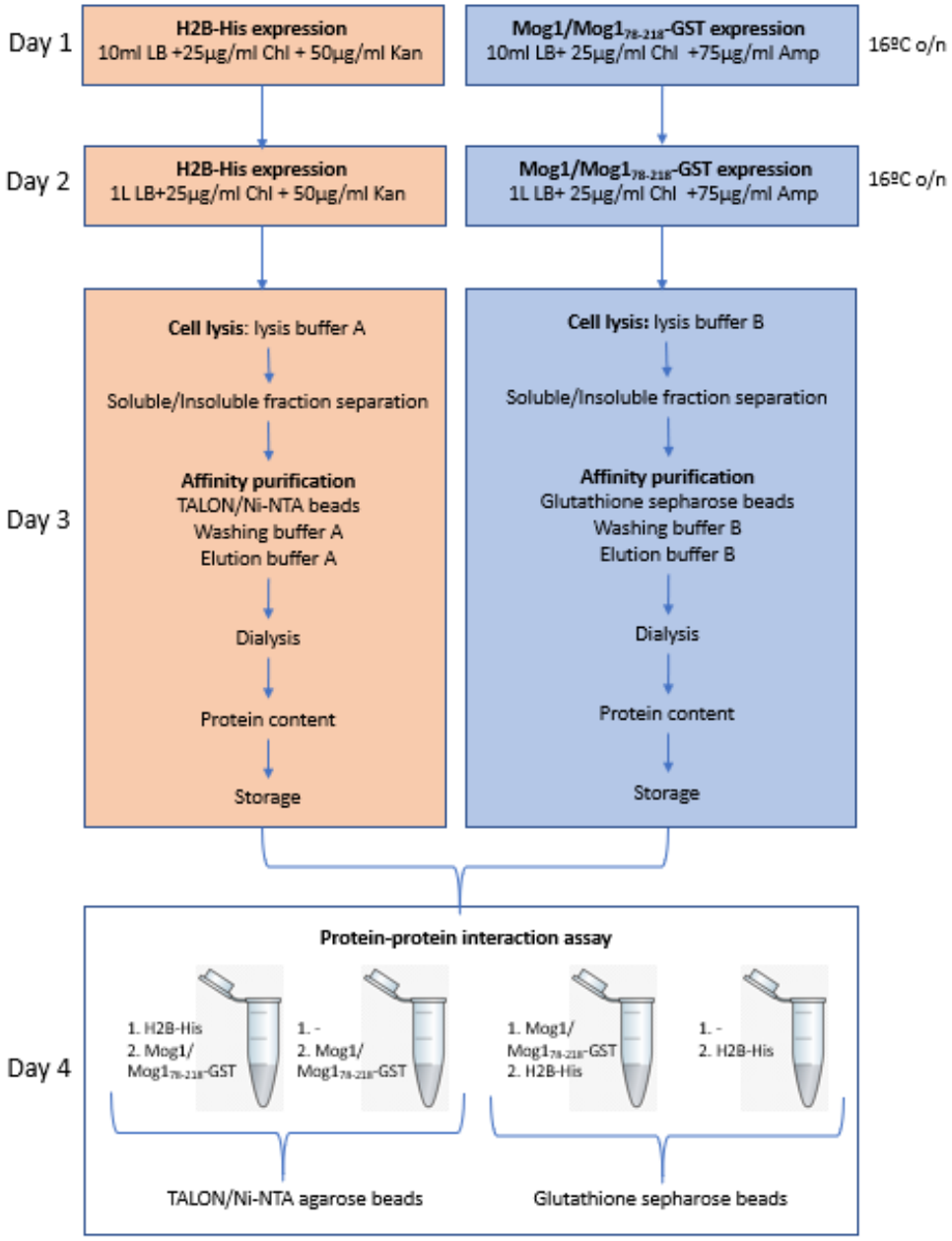

Figure 4.5. Schematic depiction of protein-protein interaction workflow.

4.5. Histone H2B-Mog1 interaction

4.5.1. IPTG induced expression of His-tagged H2B and purification by IMAC

pET28b-*HTB1*(#324) was recovered from DH5α *E. coli* cells following the protocol described in Materials and Methods, 3.4. Then, the quantity and quality of the plasmids were measured by Nanodrop to confirm that the plasmid concentration was over 100 μg/μl and that the curve fitted within the standards of good quality (lowest pick at 230nm/ highest pick at 260nm).

BL21-CodonPlus (DE3) competent *E. coli* cells were transformed with the plasmid according to the procedure described in Materials and Methods, 3.9.2. This strain was used because of its high transformation efficiency (1-5x107 cfu/μg DNA), lack of proteases Lon and OmpT, high-level protein expression and induction in T7 expression system under the control of Lac operon (NEW ENGLAND BIOLABS, 2020; AGILENT TECHNOLOGIES, 2015a). The expression was induced in a small volume (10ml LB+Chl+Kan) by adding 1mM IPTG which mimics allolactose and thus, allows the transcription of the lac operon, although it is not hydrolysable by β-galactosidase in contrast to allolactose (Marbach and Bettenbrock, 2012). The expression time was set up to 4h at 37ºC in growing cells and samples were taken before and after induction to check protein content upon IPTG induction as well as samples from soluble and insoluble fractions obtained after sonication (Materials and Methods, 3.9.3). All samples were run in a 15% SDS-PAGE (Appendix, Figure 8.7A). This showed that the induction was effective because of the appearance of a specific band of ≈15075.17kD (Gasteiger et al. 2005) in the samples obtained after induction. However, the presence of the band in the insoluble fraction revealed that histone H2B was insoluble probably aggregated in inclusion bodies.

Once the IPTG-induced expression was checked, the cell cultures were scale up to 1L volume as described in Materials and Methods 3.9.4, growing the cells for 4h at 37ºC. However, before proceeding with cell lysis, the expression of H2B was confirmed again taking samples before and after adding IPTG and running a 15% SDS-PAGE gel finding that induction worked properly (Appendix, Figure 8.7B).

To purify H2B, it was necessary to recover it from inclusion bodies, therefore the same procedure as in Materials and Methods 3.10.1 was followed but using instead the pellet obtained after sonication and centrifugation and purifying under denaturing conditions. For that, 8M urea was added to both the washing and the elution buffers to solubilise inclusion bodies following the protocol described by Tanaka et al. (2004). Approximately 25ml of the solubilised insoluble fraction were added to the column containing TALON beads. All the samples taken during the procedure were also run in a 15% SDS-PAGE (Appendix, Figure 8.8). It was obtained that H2B was correctly denatured and solubilised after the treatment with 8M urea because of the presence of an intense band at ≈15075.17kD in the treated insoluble fraction (named Sol 2). However, the same band was present in the flow through while there was no band in any of the eluates meaning that H2B did not bind to the TALON column.

Therefore, it was suggested the hypothesis that H2B was not tagged with the histidine tail in contrast to what was indicated by the plasmid provider. Therefore, the plasmid pET28b-*HTB1* was sequenced using a primer named *A3-HTB1* designed to anneal 100bp away from the 3' end of the *HTB1* gene sequence (Materials and Methods, Table 3.6). pET28b contains two His6-tag coding sequences, one located 140bp-158bp and the other one 269-277bp from the 5' end. According to the information provided with the plasmid, the *HTB1* gene was cloned between XhoI (148bp) and NcoI (295bp) restriction sites (Appendix, Figure 8.9), and thus, it was expected to find only the His6-tag coding sequence located 140-158bp in our plasmid because the other was deleted when cloning the gene (Appendix, Figure 8.10).

The sequence was aligned to the sequence of the *HTB1* gene from SGD (Cherry et al. 2012) using the sequence analysis program ApE. The alignment showed that the *HTB1* gene in the plasmid conserved the stop codon even though it was followed at 3' by the sequence coding the His6-tag (Appendix, Figure 8.11). Therefore, the encoded H2B protein was not tagged with the polyhistidine tail being unable to be purified by affinity chromatography.

It was decided to delete the stop codon (TAA) of the His-tagged *HTB1* gene in pET28b-*HTB1* by site-directed mutagenesis using the quick-change technique as detailed in Materials and Methods, 3.12. The stop codon was deleted in the three conditions tested because of the presence of a band between 5000 and 6000bp which corresponds to the plasmid size (5368bp), while there was no band in any of the controls (Appendix, Figure 8.12).

To clean the samples from the unmuted plasmid, they were treated with DpnI, which is a restriction enzyme that cleaves only when its restriction site is methylated, thus, producing the cleavage of the plasmid without the mutation which is the one containing methyl groups (Materials and Methods, 3.12.3). Then, DH5α competent *E. coli* cells were transformed with the DpnI treated samples (Materials and Methods 3.12.4) in order to circularise and amplify the plasmid for sequencing (Materials and Methods 3.11). In addition, to check that the His6-tag could be expressed, BL21-CodonPlus (DE3) competent *E. coli* cells were transformed and His6-tag expression was analysed by immunoblotting (Materials and Methods 3.12.5). Sequencing showed that the stop codon was deleted from the pET28b-*HTB1* plasmid, now being the Hi6-tag in frame attached to the 3' of the *HTB1* gene (Appendix, Figure 8.13). In addition, immunoblotting revealed that the His6-tail was properly expressed at the N-terminal of H2B (Appendix, Figure 8.14).

Once we obtained a pET28b plasmid containing the *HTB1* gene properly tagged at 3' with a histidine tail, the expression of His-tagged H2B protein was induced as explain in Materials and Methods 3.9. This time the expression was induced at 16ºC o/n since these conditions are less stringent for protein production, likely reducing protein aggregation in inclusion bodies. The expression test revealed that milder protein production conditions help to produce soluble H2B-His since there was a band of ≈15075.17kD in the soluble fraction although the overall protein content is reduced because of the lower intensity of the bands (Figure 4.6A). When scaling up, H2B-His content in the soluble fraction is significantly lower than in the insoluble one (Figure 4.6B) but we decided to purify the protein from the soluble fraction to avoid denaturation and later renaturation of the protein, thus reducing the overall duration and the complexity of the procedure.

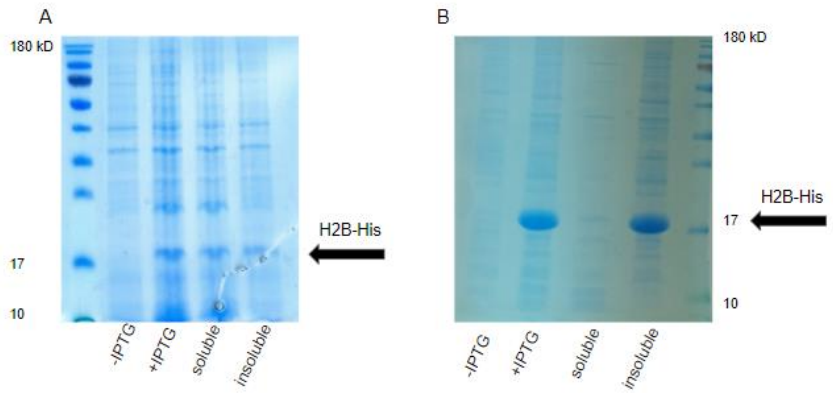

Figure 4.6. His-tagged H2B induced expression with 1mM IPTG at 16ºC o/n. *A) Expression test from 10ml of cell culture. B) Expression test from 1L of cell culture. Protein samples analysed in a 15% SDS-PAGE gel. Growth media used was LB+Chl+Kan.*

His-tagged H2B was properly purified from the soluble fraction (approximately 25ml) with a TALON column (Materials and Methods, 3.10.1) finding the higher protein content in eluates 2-5 (Figure 4.7).

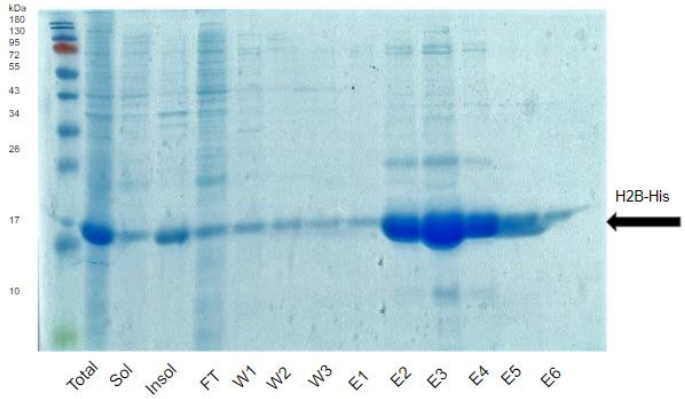

***Figure 4.7. His-tagged H2B purification by affinity chromatography using a TALON column**. Samples from each step of the procedure were taken including flow-through (FT), three washing steps (W1, W2, W3) and six elutions (E1, E2, E3, E4, E5 and E6), apart from the total, soluble and insoluble fractions and run in a 15% SDS-PAGE gel.*

Eluates E2-E5 were mixed and dialysed (Materials and Methods 3.10.1), and the protein content was quantified after dialysis by Bradford assay, obtaining a concentration of 7.06 mg/ml. Finally, the dialysed sample was aliquoted in samples of 100µL, rapidly frozen and kept at -80ºC until use.

4.5.2. IPTG induced expression of GST-tagged Mog1 and purification by Glutathione Sepharose Chromatography

pGEX4T-1-*MOG1*-GST was extracted from DH5α *E. coli* cells as explained in Materials and Methods 3.4 and the quality and quantity of plasmid was checked by Nanodrop before transforming BL21-CodonPlus (DE3) competent *E. coli* cells and inducing expression. The expression was induced following the same procedure as with His-tagged H2B (16ºC o/n), although Mog1 is a globular soluble protein that is not expected to aggregate in inclusion bodies. Mog1-GST was properly induced both in a small culture volume (Figure 4.8A) and scale-up (Figure 4.8B) as indicated by the presence of a band at ≈51275.70kD (Gasteiger et al. 2005) after IPTG induction. The presence of this band in the insoluble fraction during the test in small volume culture but not when scaling-up is probably due to an inefficient cell lysis during the first expression test (Figure 4.8).

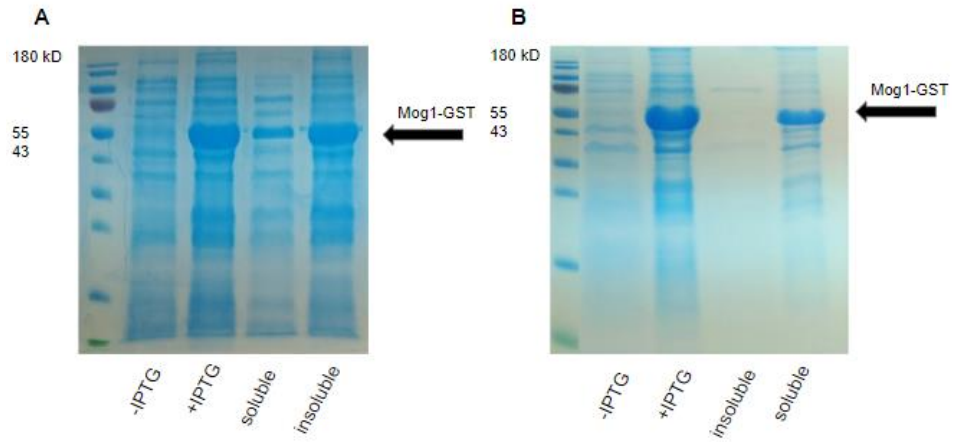

Figure 4.8. GST-tagged Mog1 induced expression with 1mM IPTG at 16ºC o/n. *A) Expression test from 10ml of bacterial culture. B) Expression test from 1L of bacterial culture. Samples were analysed in a 12% SDS-PAGE gel. Growth media used was LB+Chl+Amp.*

The soluble fraction from the scale-up culture (approximately 25ml) was filtered and used to purify the protein in a glutathione sepharose column (Materials and Methods, 3.10.2). Mog1-GST was purifed obtaining the highest protein content in the first four elution steps (Figure 4.9). These samples were dyalised obtaining a final protein content of 29,97mg/ml determined by Bradford assay. The protein containing solution was frozen in aliquotes of 100µL and kept at -80ºC.

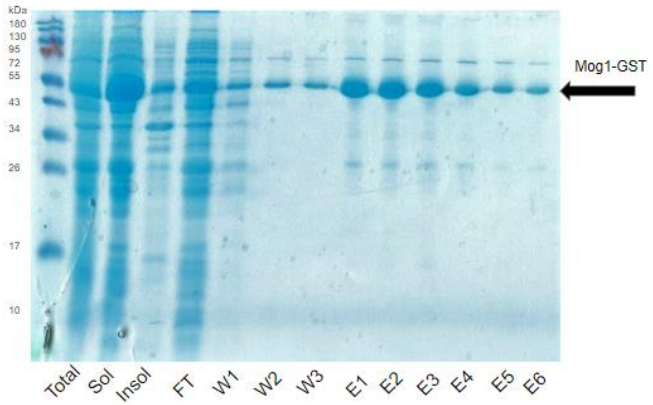

Figure 4.9. GST-tagged Mog1 purification by affinity chromatography using a glutathion sepharose column*. Samples from each step of the procedure were taken including flow-through (FT), three washing steps (W1, W2, W3) and six elutions (E1, E2, E3, E4, E5 and E6), apart from the total, soluble and insoluble fractions and run in a 12% SDS-PAGE gel.*

4.5.3. Pull-down assay for histone H2B-Mog1 interaction

Once His-tagged H2B and GST-tagged Mog1 were purified, their interaction was tested in a doble assay using: i) His-tagged H2B as the bait with TALON beads (Figure 4.10, left image) and ii) GST-tagged Mog1 as the bait instead with glutathione sepharose beads (Figure 4.10, right image). In each case, as controls the pray protein was proved for unspecific interaction with the beads, obtaining that GST-tagged Mog1 had some degree of unspecific interaction with the TALON beads and His-tagged H2B with glutathione sepharose beads. However, in both assays His-tagged H2B and GST-tagged Mog1 co-eluted. In addition, the stoichiometry of the interaction does not seem to be 1:1 being more intense the band of His-tagged H2B than that of GST-tagged Mog1 in both assays. (Figure 4.10).

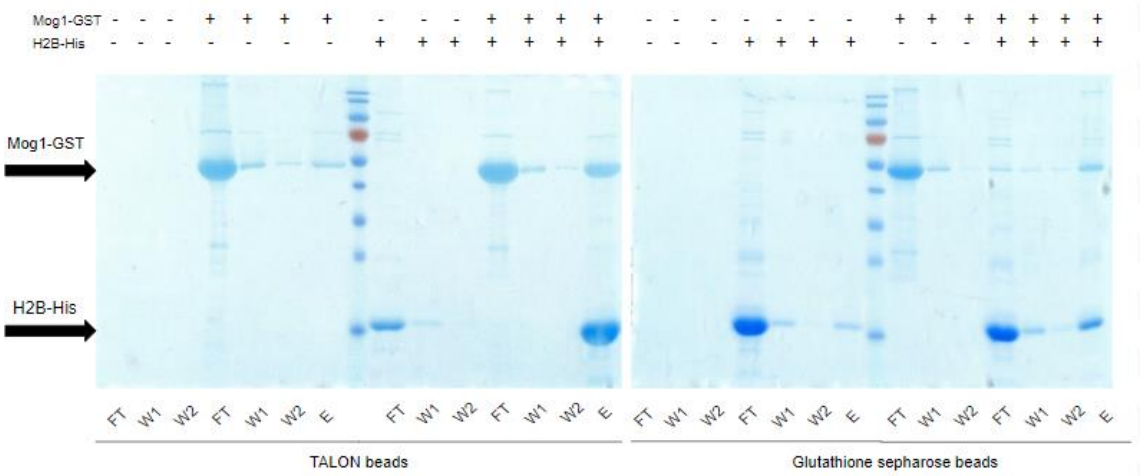

Figure 4.10. His-tagged H2B and GST-tagged Mog1 pull-down assay. *Samples from the flow through (FW), two washing steps (W1-2) and elution from each experiment were run in denaturing 12% SDS-PAGE gels. Equimolar concentrations of the pray and bait proteins were used in each assay.*

4.6. Histone H2B-Mog1 $_{78\text{-}218}$ interaction

4.6.1. IPTG induced expression of His-tagged H2B and GST-tagged Mog1$_{78\text{-}218}$

Mog1$_{78\text{-}218}$ is a shorter version of Mog1 protein lacking the Ran binding domain (28-67aa, see Introduction). By testing the interaction between this version of Mog1 and H2B, information will be gain about the putative interaction domain of these two proteins. To produce H2B-His protein again and Mog1$_{78\text{-}218}$-GST, it was proceeded as previously, using pET28b-*HTB1* (#644) and pGEX4T-*Mog1$_{78\text{-}218}$*-GST plasmids (Materials and Methods, Table 3.6) first testing the expression in a small volume of BL21-CodonPlus (DE3) competent *E. coli* cell culture and once expression was confirmed (Figure 4.11), scaling-up the expression to 1L per protein (Figure 4.12). The expression test from 10ml of cell culture revealed that both proteins were expressed by adding 1mM IPTG because of the presence of a band at ≈42595.05kD (Gasteiger et al. 2005) corresponding to Mog1$_{78\text{-}218}$-GST and a band at ≈15075.17kD, corresponding to H2B-His. However, this time expression was less efficient than in the previous experiments, especially in the case of Mog1$_{78\text{-}218}$-GST. GST-tagged Mog1$_{78\text{-}218}$ was mostly expressed in the soluble fraction while His-tagged H2B in the insoluble one (Figure 4.11). When scaling up the production, the expression of both proteins was higher, increasing histone content in the soluble fraction (Figure 4.12).

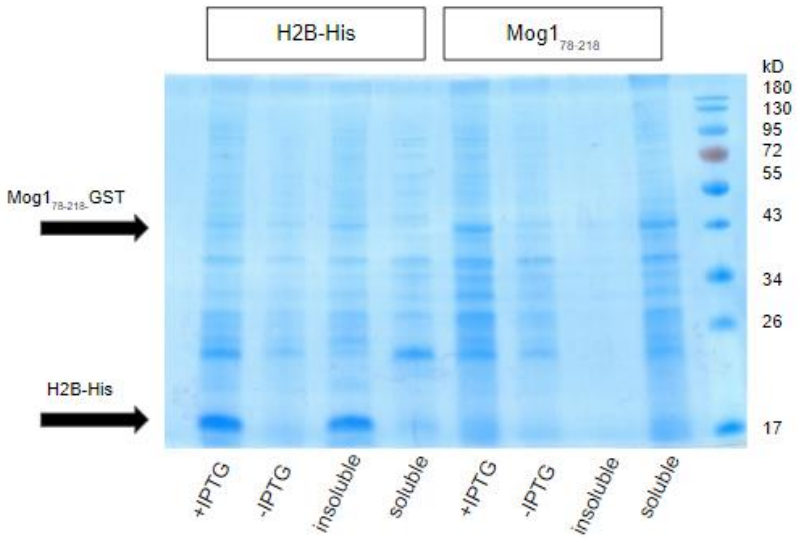

Figure 4.11. H2B-His and Mog1$_{78\text{-}218}$-GST induced expression with 1mM IPTG at 16ºC o/n. *Expression test in 10ml of bacterial culture. 12% SDS-PAGE gel. For H2B-His, LB+Chl+Kan was used whereas LB+Chl+Amp for Mog1$_{78\text{-}218}$-GST.*

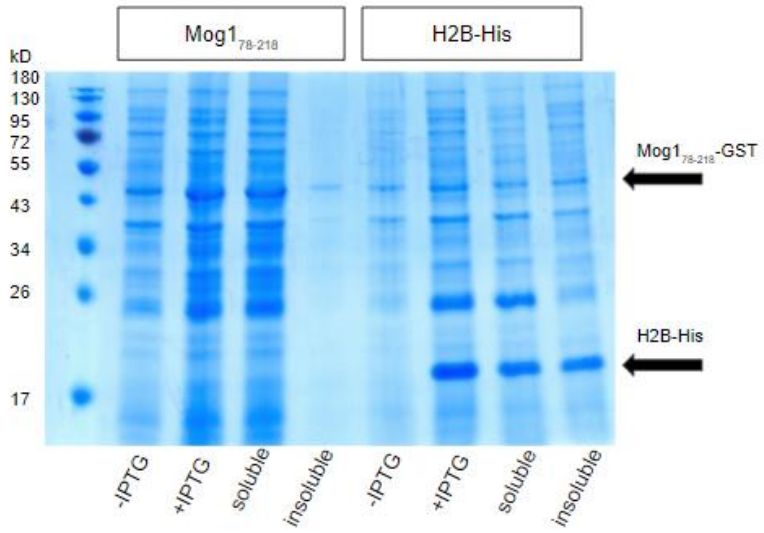

Figure 4.12. H2B-His and Mog1$_{78-218}$ -GST induced expression with 1mM IPTG at 16ºC o/n. *Expression test from 1L of bacterial culture. 12% SDS-PAGE gel. For H2B-His, LB+Chl+Kan was used, whereas LB+Chl+Amp for Mog1$_{78-218}$ -GST.*

4.6.2. His-tagged H2B purification by IMAC

In this case, His-tagged H2B was purified from the soluble fraction (approximately 25ml) by using niquel-nitriloacetic acid (Ni-NTA) agarose beads (HisPur™ Ni-NTA Resin, ThermoScientific®) instead of TALON beads. Most of the protein was eluted in steps 2 and 3, and to a lesser extent, 4 (Figure 4.13). Nevertheless, the presence of other bands of different size in the eluates 2 and 3 indicated that other proteins were purified together with our protein and thus, the samples were not pure enough for a protein-protein interaction assay. Therefore, only elute 4 was dialysed, aliquoted and frozen, being the protein concentration 1.5mg/ml as determined by Bradford assay.

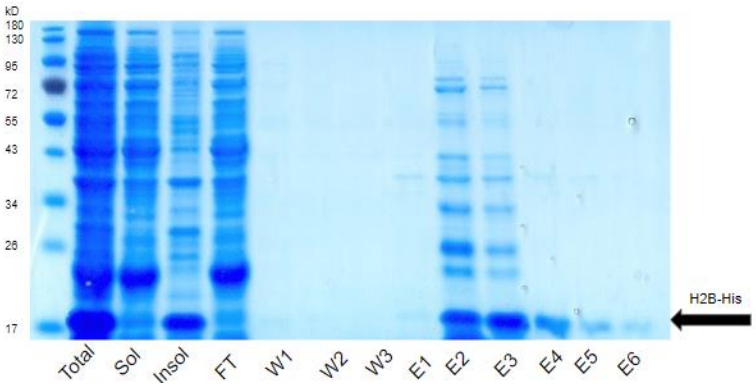

Figure 4.13. His-tagged H2B purification by affinity chromatography using a Ni-NTA agarose column*. Samples from each step of the procedure were taken including flow-through (FT), three washing steps (W1, W2, W3) and six elutions (E1, E2, E3, E4, E5 and E6), apart from the total, soluble and insoluble fractions and run in a 15% SDS-PAGE gel.*

4.6.3. GST-tagged Mog1$_{78-218}$ purification by Gluthathione Sepharose Chromatography

Mog1$_{78-218}$-GST was purified from the soluble fraction (≈25ml) with glutathione sepharose beads (Materials and Methods, 3.10.2) as in the case of GST-tagged Mog1. Although the protein content seemed lower when checking the expression compared to Mog1-GST, after purification intense

bands at ≈42595.05kD were obtained in the six eluates, being significantly more intense and wider in eluates 2 and 3 (Figure 4.14). However, as in H2B-His purification, these fractions contained contaminants that co-purified with Mog1$_{78-218}$-GST making these fractions not suitable for a protein-protein interaction assay. Therefore, the protein content of the other eluates was measured by Bradford assay and only the eluate 4 which had the highest protein content (6.97 mg/ml), was dialysed, aliquoted and frozen.

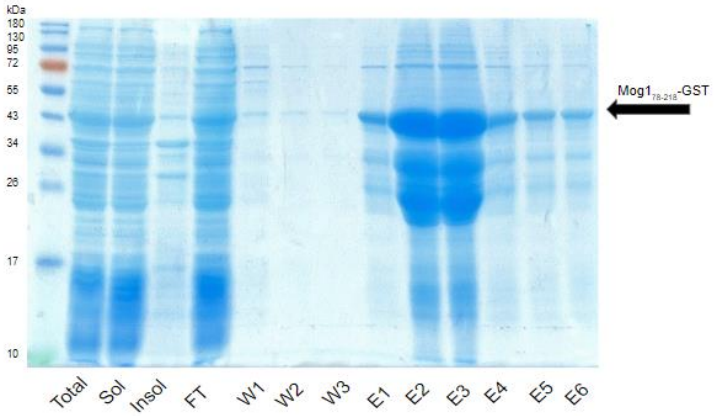

Figure 4.14. GST-tagged Mog1$_{78-218}$ purification by affinity chromatography using a glutathion sepharose column*. Samples from each step of the procedure were taken including flow-through (FT), three washing steps (W1, W2, W3) and six elutions (E1, E2, E3, E4, E5 and E6), apart from the total, soluble and insoluble fractions and run in a 12% SDS-PAGE gel.*

4.6.4. Pull-down assay for histone H2B- Mog1$_{78-218}$ interaction

H2B-Mog1$_{78-218}$ binding was tested in both directions: i) by using His-tagged H2B as the bait and Ni-NTA agarose beads (Figure 4.15, left) and ii) by using glutathione sepharose beads and GST-tagged Mog1$_{78-218}$ as the bait (Figure 4.15, right). As seen in H2B-Mog1 interaction assay, unspecific H2B-His interaction with glutathione sepharose beads as well as Mog1$_{78-218}$-GST with Ni-NTA agarose beads was detected. Also, in both assays, the proteins co-eluted although in this case the purity of the Mog1$_{78-218}$-GST sample was not good enough due to presence of other bands at the Mog1$_{78-218}$-GST fraction (Figure 4.15).

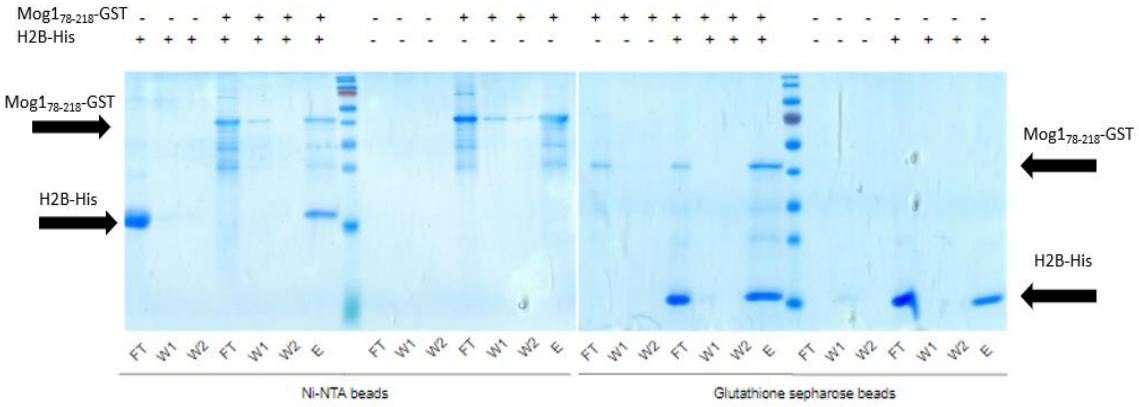

Figure 4.15. His-tagged H2B and GST-tagged Mog1$_{78-218}$ pull-down assay. *Samples from the flow through (FW), two washing steps (W1-2) and elution from each experiment were run in denaturing 12% SDS-PAGE gels. Equimolar concentrations of the pray and bait proteins were used in each assay.*

5. DISCUSSION

5.1. Phenotypic effect of Mog1W145A and Mog1E65KW145A mutations in *mog1Δ* and *set1Δmog1Δ S. cerevisiae* growth

Defective growth caused by gene deletions is usually restored by introducing a plasmid with the wild type version of the gene of interest. However, in the case of Mog1, plasmid complementation was only partial in both *mog1Δ* or *set1Δmog1Δ* mutant strains as seen by growth assay and by growth curves. This might be due to specific mRNA structures avoiding access to transcription machinery and properly folding, reducing the stability of the protein which, in turn, can reduce protein availability and protein content due to protein degradation. Therefore, the phenotype of the complemented strain will be used as the reference to analyse the phenotypic effects of Mog1 mutations since it represents how the wild type Mog1 is expressed from a plasmid.

In addition, it is also relevant to consider the characteristics of the mutant strains. The phenotype of *mog1Δ* suggests that the Mog1 protein is important for cell viability and its deletion makes yeast temperature sensitive for growth, which has been also reported in other studies (Oki and Nishimoto, 1998). Notably, Mog1 is essential in other yeast species as for instance *S. pombe* (Tatebayashi et al. 2001). In *set1Δmog1Δ*, the lack of *SET1* compromises cell viability because it performs important cellular functions. As explained in the introduction of this work, Set1 is the catalytic subunit of COMPASS complex, responsible for mono-, di- and trimethylation of histone H3 at K4 which, in turn, is involved in transcription elongation regulation (see Introduction), telomeric silencing (Nislow et al. 1997; Corda et al. 1999) and other processes as for instance meiosis (Miller et al. 2001; Govindaraghavan et al. 2014). Therefore, the deletion of both *SET1* and *MOG1* leads to a synthetically sick phenotype as seen both by growth assays and growth curves.

In *mog1Δ* strain, either single point mutations E65K and W145A or double point mutation E65KW145A do not have any phenotypic effect compared to that showed by *mog1Δ*+pMog1 at 30ºC, which is the optimal growth temperature. However, what it is interesting is the effect of these mutations at 37ºC since one would expect a slower growth phenotype because of the temperature sensitive growth showed by both *mog1Δ* and *mog1Δ*+pMog1 strains. In contrast, mutations complement growth better than *mog1Δ*+pMog1. This could be explained in terms of protein stability. It could be that, if wild type Mog1 is less stable because of unproper folding when expressed from a plasmid, these point mutations in Mog1 might help to stabilise the protein, increasing the amount of functional protein available for the function or functions that are not impaired by each mutation. In case of the double mutant E65KW145A, in which Mog1 functions in nuclear protein import and mRNA transcription are thought to be unpaired, this would imply that Mog1 might have other functions probably more evident during stress conditions.

This hypothesis gains weight when analysing the effects of the mutations in *set1Δmog1Δ* mutant strain. At 30ºC, mutations show the same phenotype as in *mog1Δ* mutant strain at 30ºC. However, at 37ºC the behaviour is very different than that seen in *mog1Δ.* E65K point mutation causes a slower growth phenotype compared to *set1Δmog1Δ*+pMog1 while W145A point mutations leads to a synthetically sick phenotype, suggesting that when important cellular functions are impaired and cells are stressed, increasing Mog1p stability is not sufficient to rescue the phenotype. However, the double mutation E65KW145A has a positive effect on growth. This could reflect a higher stability under these conditions than that of the single mutants and fully availability of Mog1 to perform other functions essential for cell viability. These putative new functions are likely related to stress response mechanisms and pushing the balance of Mog1 towards these functions seems to benefit the cell.

5.2. Phenotypic effect of Mog1ΔK144-T153 and Mog1K189A mutations in *mog1Δ* and *set1Δmog1Δ S. cerevisiae* growth

Growth curves should be analysed also considering what has been explained about Mog1 complementation and *mog1Δ* and *set1Δmog1Δ* mutant strains. In a *mog1Δ* mutant strain, the K189A mutation and deletion of the K144-T153 loop reduce slightly the growth rate compared to *mog1Δ*+pMog1. This suggests that these residues might be either important for Mog1 stability or Mog1 function. Nevertheless, when analysing *set1Δmog1Δ* mutant strain the effects on growth of these mutations are totally different. Both mutations have a positive effect on *set1Δmog1Δ* growth, complementing growth better than *set1Δmog1Δ*+pMog1 at both temperatures. The effect of K189A mutation is especially interesting since it increases the growth rate of *set1Δmog1Δ* almost to *set1Δ* at 30ºC, surpassing it at 37ºC. It is also significant that the growth rates of the *set1Δmog1Δ* strains bearing these mutations are higher at 37ºC than at 30ºC, meaning that these mutations in the Mog1 protein are somehow improving the growth of the cells under temperature stress and in an unfavourable cellular environment. This might be also explained in terms of protein stability. By deleting the loop K144-T153, both the structure and function of Mog1 could be affected, improving stability on the one hand, and impairing Mog1 binding to Shg1 on the other hand, therefore, making the protein more available for other functions that might be more necessary for cell viability. Assuming our hypothesis of Mog1 involvement in stress response mechanisms, this changes in Mog1 would be important especially in the case of the defective strain *set1Δmog1Δ*. Regarding K189A Mog1 mutation, preventing putative K189 mono/polyubiquitylation could prevent protein degradation since K189 mono/polyubiquitylation might be a target site for degradation. A study found that contrary to what was thought, H2B is extensively polyubiquitylated and not only monoubiquitylated, and it seems that these PTMs are driven by different mechanisms (Geng and Tansey, 2008). Reducing Mog1 degradation could lead to protein accumulation and cellular toxicity, in case of *mog1Δ* strain, while in the case of *set1Δmog1Δ* mutant strain, the protein availability and content are important if Mog1 is involved in stress response mechanisms, which fits well with the results discussed in the previous section.

Regarding the growth rate and doubling time values estimated, some studies have reported that the doubling time of the *S. cerevisiae* BY4741 wild type strain is approximately 90 min when optimal growing conditions are applied, pH=4 and DO= 5% (Kaeberlein, 2010; Salari and Salari, 2017). The doubling time calculated in our experiments for BY4741 wild type strain almost doubles the expected. This can be explained by the growth conditions during the measurement of OD_{600} in the microplates where cell cultures in the wells of the microplate do not accomplish the medium-vessel proportion of 1:5 to assure aeration, and shaking is not continuous.

5.3. Histone H2B-Mog1 interaction

Protein overexpression and purification is not an easy and simple procedure, especially when producing recombinant histones. These small basic proteins are insoluble in physiological conditions and require histone chaperons for acquiring their native structure (Akey and Luger, 2003). Histone proteins purified from homologous cell extracts are heterogeneous because there are isoforms with minor sequence differences that can bear sequence dependent posttranslational modifications (Wallis et al. 1980; Kamakaka and Biggins, 2005; Henikoff and Smith, 2015). In addition, the proteolytic products that accumulate during isolation can contaminate the protein extract (Urban et al. 1979). Bacterially expressed histones are not post-translationally modified, obtaining high homogeneous protein content that should limit proteolytic degradation (Tanaka et al. 2004). Actually, a nucleosome core particle has been reconstituted from *E. coli* expressed histones of *Xenophus laevis* (Luger at al. 1997b; Luger et al. 1999, Lee et al. 2015) and more recently, human histones were expressed and purified in *E. coli* (Tanaka et al. 2004). However,

when proteins are overexpressed in *E. coli*, the rate of protein proper folding is often much lower than that of protein aggregation because chaperons are rapidly used and heat shock proteins are induced, therefore, proteins can aggregate and form inclusion bodies, although this event depends on protein stability and conditions during induced expression (Chesshyre and Hipkiss, 1989; Clark, 2001). Inclusion bodies are protein aggregates that can be found in the cytoplasm of bacteria and it has been reported that when histones are expressed individually, they end up forming inclusion bodies (Luger et al. 1997b, Tanaka et al. 2004; Anderson et al. 2010¸ Shim et al. 2012; Lee et al. 2015; Ivić et al. 2016).

Consequently, several strategies have been developed to either minimize histone aggregation in inclusion bodies or to recover histones from them. Regarding the first approach, it has been proposed to reduce gene expression rates by lowering the culture temperature to 16-20ºC (Ivić et al. 2016), to coproduce histone chaperons together with histones (Anderson et al. 2010), to co-express the histone dimer H2A-H2B and tetramer $(H3\text{-}H4)_2$ (Anderson et al. 2010, Ivić et al. 2016) or even including the four histone genes in a polycistronic vector (Shim et al. 2012). The second approach involves recovering inclusion bodies to transform aggregated recombinant histones into the active soluble form by solubilisation and refolding. Histones can be solubilised from inclusion bodies by adding denaturing agents such as guanidine hydrochloride or urea and refolding later by first removing denaturants through dialysis (Yamaguchi and Miyazaki, 2014) and later mixing the unfolded histones together (Luger et al. 1999, Tanaka et al. 2004, Lee et al. 2015). However, the efficiency and success of these procedures is variable and unpredictable (Rinas et al. 2017).

Furthermore, even when obtaining high expression levels of soluble protein, purification is not trivial, especially when high purity is necessary for a protein-protein interaction assay (Phizicky and Field, 1995). Histone H2B was purified using TALON beads, an immobilized metal affinity chromatography (IMAC) resin charged with cobalt, which is highly specific for His-tagged proteins, obtaining 100-fold enrichments in a single purification step (TAKARA BIO, 2018). However, since other proteins in the cell extracts can have two or more adjacent histidine residues in their sequence, 20mM imidazole, a natural analogue of histidine, and a high salt concentration (500mM) was added to the washing and elution buffers (see Materials and Methods, 3.10.1) to reduce unspecific binding. Also, the addition of 10mM 2-mercaptoetanol, Triton X-100, Tween 20, up to 20% glycerol or low levels of ethanol (up to 20%) to the washing and elution buffers is commonly used for this purpose (Bornhorst and Falke, 2000). In the case of Mog1 purification in glutathione sepharose columns, unspecific binding is less likely because of the nature of the GST tag, a naturally occurring 26kDa protein found in eukaryotic cells (Harper and Speicher, 2011). However, in histone H2B-Mog1 protein-protein interaction assay both His-tagged H2B interacted with the glutathione sepharose column and GST-tagged Mog1 with the TALON column. One could expect that Mog1-GST could interact with TALON column because of the presence of two or more adjacent histidine residues either in Mog1 protein or GST, but this is not case. In addition, this would not explain why H2B-His also bound to the glutathione sepharose column. Otherwise, unspecific binding happened likely because too many beads were used for the pull-down assay, leaving more empty space for the proteins to directly adsorb to the resin. To prevent this in further experiments, one could try to reduce the volume of beads used or add BSA (Bovine Serum Albumin) as a blocking agent (Bornhorst and Falke, 2000). If unspecific binding is still detected, it could be useful to change the columns used or even the affinity tags.

Despite the unspecific binding, when comparing the intensity of the bands in the eluates between the controls and its corresponding interaction assay, we can suggest that Mog1 and histone H2B interact. In both cases, the band corresponding to the fraction of pray protein binding non-specifically to the beads is significantly less intense that the band corresponding to the pray protein when co-eluted with the bait, even though this putative interaction should be counteracted in further experiments. On the one hand, with the aim of reassembling more the physiological

state of the proteins, GST tag should be cleaved from Mog1 since the plasmid contains a protease cleavage site for thrombin between GST and the 3' of *MOG1*, testing again the interaction between Mog1 and H2B. In the case of H2B, the relatively small size and charge of the His6 tag makes its cleavage unnecessary. On the other hand, it would be very informative to determine the affinity of the interaction. For that, there exists several techniques such as biolayer interferometry, which is an optical analytical technique that analyses the shift in the interference pattern when a protein interacts with another protein immobilised on a biosensor tip (Shah and Duncan, 2014). The affinity of the interaction can also be quantified by measuring shifts in protein stability upon binding which is called thermal sift assay or thermofluor (Layton and Hellinga, 2011; Bai et al. 2019) or by white light scattering applied to a chromatographic separation method (GC-MALS or SEC-MALS) (Some, 2013). MALS also gives information about the absolute stoichiometry of the interaction, making MALS a good choice because H2B-Mog1 interaction seemed not to be 1:1 since the intensity of the H2B-His band is significantly higher than that of Mog1-GST band when co-eluted in both assays. This suggests that several units of H2B could bind to a single Mog1 protein. For this purpose, blue native PAGE gels are commonly used but it is not appliable in this case because on one hand, the high isoelectric point of H2B-His tagged (pI= 10.10, Gasteiger et al. 2005) prevents histones to enter into gel and run towards the anode and, on the other hand, the isoelectric point of GST-tagged Mog1 is 5.10 (Gasteiger et al. 2005), therefore it is not possible to adjust the pH of the running buffer so it is suitable for both proteins since pI<pH (Wittig et al. 2006).

5.4. Histone H2B-Mog1$_{78\text{-}218}$ interaction

Apart from the difficulties found when overexpressing recombinant histones in *E. coli* discussed in the previous section, one must face with non-consistent protein expression. When comparing induced expression of H2B-His and Mog1-GST in the first assay to H2B-His and Mog1$_{78\text{-}218}$-GST in the second one, protein production is less efficient in this last assay although applying the same induction and growth conditions. This problem has been reported elsewhere and it has to do with the bacterial expression system used, BL21-CodonPlus (DE3) *E. coli*. This strain expresses T7 RNA polymerase at a high basal level, therefore proteins are often expressed before induction. This is a problem when the protein is toxic for the cell which can be noticed by the presence of colonies of different size when plating cells after transformation. This can be avoided by using BL21(DE)pLysS *E. coli* cells since T7 lysozyme which naturally inhibits T7 RNA polymerase is expressed in the plasmid pLysS providing tight promotor control. Moreover, it is recommended not to maintain the colonies plated more than one week before inducing expression (NEW ENGLAND BIOLABS, 2011; AGILENT TECHNOLOGIES, 2015a). Therefore, BL21(DE3) pLysS *E. coli* strain should be used instead in further experiments.

Once proteins were expressed, purification was not stringent enough since in both purifications the eluates with the highest protein content were significantly contaminated. In the case of the His-tagged H2B it might be due to the use of Ni-NTA column instead of TALON beads used previously. It has been suggested that TALON beads could bind to his-tagged proteins with higher specificity than nickel-charged resins (TAKARA BIO, 2018). Using the eluates from the last purifications with no or less contaminants worked for H2B-His but not for Mog1$_{78\text{-}218}$-GST since those bands also appeared during the pull-down assay. At this stage, it is not possible to conclude if H2B and Mog1$_{78\text{-}218}$ interact directly. The assay should be repeated using the highest protein content eluates after re-purification by affinity chromatography and adding more reagents that reduce unspecific binding as described in the previous section.

6. CONCLUSIONS

From the experiments performed in this project and after the analysis of the results, the following conclusions can be stated:

1. W145A and E65KW145A mutations in the Mog1 protein improve yeast cell growth at high temperatures in *mog1Δ* mutant strain but only E65KW145A mutation has this phenotypic effect in *set1Δmog1Δ* mutant strain. These mutations might increase the stability of the Mog1 protein when expressed from a plasmid in absence of genomic *MOG1* rising the amount of protein available to perform the functions that are not impaired by the mutations. This improvement of the protein stability seems to be especially important when the cells are exposed to high temperatures, suggesting that Mog1 might have other functions more evident during stress conditions. When combining *MOG1* and *SET1* deletions, the increase in stability due to W145A mutations is not enough to rescue the phenotype under stress. However, E65KW145A mutation positive effect on growth suggests that liberating Mog1 from its known functions benefits the cell, supporting the hypothesis of Mog1 participation in stress response mechanisms.
2. K144-T153 deletion and K189A mutation in Mog1 improve yeast cell growth at high temperatures when important cellular functions are also compromised, this is the case of *set1Δmog1Δ* strain. K144-T153 deletion might benefit the cell by increasing Mog1 stability and liberating Mog1 from Shg1 binding, making the protein more available to perform other functions that might be more important for cell viability. At the same time, the K189A mutation could prevent mono/polyubiquitylation at this residue which could avoid degradation of Mog1, which in turn means that more protein would be available. Altogether these results support the hypothesis of a new function of Mog1 related to stress response mechanisms.
3. Histone H2B and Mog1 protein interact *in vitro* in a stoichiometry likely different to 1:1. Further experiments should be performed to support these results and determine the stoichiometry of the interaction.
4. Direct interaction between H2B and $Mog1_{78\text{-}218}$ cannot be concluded from the experiments performed in this work and the assay should be repeated considering the aspects discussed.

7. REFERENCES

ADDGENE (2019) Plasmid: pET-28b(+). Addgene, the non-profit plasmid repository. Visited the 6th June 2019. Retrieved from: https://www.addgene.org/vector-database/2566/?gclid=CjwKCAjw3azoBRAXEiwA-_64Ov-Hy7KnsMilZDgXMNZvwOtCY0j0bGBZ3fUwVg_RKJ0x5ek55tkH2BoCUqkQAvD_BwE

AGILENT TECHNOLOGIES, LNC (2015a) BL21-CodonPlus Competent Cells Instruction Manual. Catalogue #230240, #230245, #230250, #230255, #230265, #230275 and 230280, Revision C.0. Visited the 15th January 2020. Retrieved from https://www.agilent.com/cs/library/usermanuals/public/230240.pdf

AGILENT TECHNOLOGIES, LNC. (2015b). QuikChange II Site-Directed Mutagenesis Kit Instruction Manual. Catalogue ·200523. Visited the 7th June 2019. Retrieved from: https://www.agilent.com/cs/library/usermanuals/Public/200523.pdf

AKEY, C. W., & LUGER, K. (2003). Histone chaperones and nucleosome assembly. *Current opinion in structural biology*, 13(1), 6-14.

ALLFREY, V. G., FAULKNER, R., & MIRSKY, A. E. (1964). Acetylation and methylation of histones and their possible role in the regulation of RNA synthesis. *Proceedings of the National Academy of Sciences*, 51(5), 786-794.

ANDERSON, M., HUH, J. H., NGO, T., LEE, A., HERNANDEZ, G., PANG, J., ... & DUTNALL, R. N. (2010). Co-expression as a convenient method for the production and purification of core histones in bacteria. *Protein expression and purification*, *72*(2), 194-204.

ANTZELEVITCH, C. H., BRUGADA, P., BRUGADA, J., BRUGADA, R., SHIMIZU, W., GUSSAK, I., & PEREZ RIERA, A. R. (2002). Brugada syndrome: a decade of progress. *Circulation research*, *91*(12), 1114-1118.

ANTZELEVITCH, C., BRUGADA, P., BORGGREFE, M., BRUGADA, J., BRUGADA, R., CORRADO, D., ... & SHIMIZU, W. (2005). Brugada syndrome: report of the second consensus conference: endorsed by the Heart Rhythm Society and the European Heart Rhythm Association. *Circulation*, 111(5), 659-670.

BAI, N., RODER, H., DICKSON, A., & KARANICOLAS, J. (2019). Isothermal analysis of thermofluor data can readily provide quantitative binding affinities. *Scientific reports*, 9(1), 1-15.

BAKER, R. P., HARREMAN, M. T., ECCLESTON, J. F., CORBETT, A. H., & STEWART, M. (2001). Interaction between Ran and Mog1 is required for efficient nuclear protein import. *Journal of Biological Chemistry*, 276(44), 41255-41262.

BANNISTER, A. J., & KOUZARIDES, T. (2011). Regulation of chromatin by histone modifications. *Cell research*, 21(3), 381.

BAO, X., LIU, H., LIU, X., RUAN, K., ZHANG, Y., ZHANG, Z., ... & GONG, Q. (2018). Mitosis-specific acetylation tunes Ran effector binding for chromosome segregation. *Journal of molecular cell biology*, *10*(1), 18-32.

BARTKE, T., VERMEULEN, M., XHEMALCE, B., ROBSON, S. C., MANN, M., & KOUZARIDES, T. (2010). Nucleosome-interacting proteins regulated by DNA and histone methylation. *Cell*, 143(3), 470-484.

BERGER, S. L. (2007). The complex language of chromatin regulation during transcription. *Nature*, *447*(7143), 407-412.

BLOUNT, B. A., DRIESSEN, M. R., & ELLIS, T. (2016). GC preps: fast and easy extraction of stable yeast genomic DNA. *Scientific reports*, *6*, 26863.

BORNHORST, J. A., & FALKE, J. J. (2000). Purification of proteins using polyhistidine affinity tags. *Methods in enzymology*, *326*, 245–254.

BOTSTEIN, D., CHERVITZ, S. A., & CHERRY, M. (1997). Yeast as a model organism. *Science*, 277(5330), 1259-1260.

BRÜCKNER, A., POLGE, C., LENTZE, N., AUERBACH, D., & SCHLATTNER, U. (2009). Yeast two-hybrid, a powerful tool for systems biology. *International journal of molecular sciences*, *10*(6), 2763-2788.

BRUGADA P & BRUGADA J. (1992) Right bundle branch block, persistent ST segment elevation and sudden cardiac death: a distinct clinical and electrocardiographic syndrome: a multicenter report. *J Am Coll Cardiol*. ;20: 1391–1396

CHANG, A. Y., CHAU, V. W., LANDAS, J. A., & PANG, Y. (2017). Preparation of calcium competent Escherichia coli and heat-shock transformation. *JEMI Methods*, *1*, 22-25.

CHEE, M. K. & HAASE, S. B. (2012). New and redesigned pRS plasmid shuttle vectors for genetic manipulation of Saccharomyces cerevisiae. G3: *Genes, Genomes, Genetics*, 2(5), 515-526.

CHEN, Q., KIRSCH, G. E., ZHANG, D., BRUGADA, R., BRUGADA, J., BRUGADA, P., ... & ORTIZ-LOPEZ, R. (1998). Genetic basis and molecular mechanism for idiopathic ventricular fibrillation. *Nature*, 392(6673), 293.

CHERRY, J. M., HONG, E. L., AMUNDSEN, C., BALAKRISHNAN, R., BINKLEY, G., CHAN, E. T., ... & FISK, D. G. (2012). Saccharomyces Genome Database: the genomics resource of budding yeast. *Nucleic acids research*, *40*(D1), D700-D705.

CHESSHYRE, J. A., & HIPKISS, A. R. (1989). Low temperatures stabilize interferon α-2 against proteolysis in Methylophilus methylotrophus and Escherichia coli. *Applied microbiology and biotechnology*, *31*(2), 158-162.

CLARK, E. D. B. (2001). Protein refolding for industrial processes. *Current opinion in biotechnology*, 12(2), 202-207.

CORDA, Y., SCHRAMKE, V., LONGHESE, M. P., SMOKVINA, T., PACIOTTI, V., BREVET, V., ... & GÉLI, V. (1999). Interaction between Set1p and checkpoint protein Mec3p in DNA repair and telomere functions. *Nature genetics*, 21(2), 204-208.

DEHÉ, P. M., DICHTL, B., SCHAFT, D., ROGUEV, A., PAMBLANCO, M., LEBRUN, R., ... & SHEVCHENKO, A. (2006). Protein interactions within the Set1 complex and their roles in the regulation of histone 3 lysine 4 methylation. *Journal of biological chemistry*, *281*(46), 35404-35412.

DEMAIN, A. L., & VAISHNAV, P. (2009). Production of recombinant proteins by microbes and higher organisms. *Biotechnology advances*, *27*(3), 297-306.

FIELDS, S., & SONG, O. K. (1989). A novel genetic system to detect protein–protein interactions. *Nature*, *340*(6230), 245-246.

FLEMING, A. B., KAO, C. F., HILLYER, C., PIKAART, M., & OSLEY, M. A. (2008). H2B ubiquitylation plays a role in nucleosome dynamics during transcription elongation. *Molecular cell*, *31*(1), 57-66.

FORMOSA, T., RUONE, S., ADAMS, M. D., OLSEN, A. E., ERIKSSON, P., YU, Y., ... & STILLMAN, D. J. (2002). Defects in SPT16 or POB3 (yFACT) in Saccharomyces cerevisiae cause dependence on the Hir/Hpc pathway: polymerase passage may degrade chromatin structure. *Genetics*, *162*(4), 1557-1571.

FOURY, F. (1997). Human genetic diseases: a crosstalk between man and yeast. *Gene*, 195(1), 1-10.

FUCHS, G., & OREN, M. (2014). Writing and reading H2B monoubiquitylation. *Biochimica et Biophysica Acta (BBA)-Gene Regulatory Mechanisms*, *1839*(8), 694-701.

GASTEIGER, E., HOOGLAND, C., GATTIKER, A., WILKINS, M. R., APPEL, R. D., & BAIROCH, A. (2005). Protein identification and analysis tools on the ExPASy server. In *The proteomics protocols handbook* (pp. 571-607). Humana press.

GENG, F., & TANSEY, W. P. (2008). Polyubiquitylation of histone H2B. *Molecular biology of the cell*, 19(9), 3616-3624.

GIANNATTASIO, M., LAZZARO, F., PLEVANI, P., & MUZI-FALCONI, M. (2005). The DNA damage checkpoint response requires histone H2B ubiquitination by Rad6-Bre1 and H3 methylation by Dot1. *Journal of Biological Chemistry*, *280*(11), 9879-9886.

GIETZ, R. D., & SCHIESTL, R. H. (2007). High-efficiency yeast transformation using the LiAc/SS carrier DNA/PEG method. *Nature protocols*, *2*(1), 31-34.

GOFFEAU, A., BARRELL, B. G., BUSSEY, H., DAVIS, R. W., DUJON, B., FELDMANN, H., ... & LOUIS, E. J. (1996). Life with 6000 genes. *Science*, 274(5287), 546-567.

GOVINDARAGHAVAN, M., ANGLIN, S. L., OSMANI, A. H., & OSMANI, S. A. (2014). The Set1/COMPASS histone H3 methyltransferase helps regulate mitosis with the CDK1 and NIMA mitotic kinases in Aspergillus nidulans. *Genetics*, 197(4), 1225-1236.

HANAHAN, D. (1983). Studies on transformation of Escherichia coli with plasmids. *Journal of molecular biology*, 166(4), 557-580.

HARPER, S., & SPEICHER, D. W. (2011). Purification of proteins fused to glutathione S-transferase. *Methods in molecular biology (Clifton, N.J.)*, *681*, 259–280.

HENIKOFF, S., & SMITH, M. M. (2015). Histone variants and epigenetics. *Cold Spring Harbor perspectives in biology*, 7(1), a019364.

HENRY KW, WYCE A, LO W-S, DUGGAN LJ, EMRE NCT, KAO C-F, PILLUS L, SHILATIFARD A, OSLEY MA, BERGER SL (2003) Transcriptional activation via sequential histone H2B ubiquitylation and deubiquitylation, mediated by SAGA-associated Ubp8. *Genes Dev* 17: 2648 – 2663

HÉRISSANT, L., MOEHLE, E. A., BERTACCINI, D., VAN DORSSELAER, A., SCHAEFFER-REISS, C., GUTHRIE, C., & DARGEMONT, C. (2014). H2B ubiquitylation modulates spliceosome assembly and function in budding yeast. *Biology of the Cell*, *106*(4), 126-138.

HERSHKO, A., & CIECHANOVER, A. (1998). The ubiquitin system. *Annual review of biochemistry*, *67*(1), 425-479.

INGVARSDOTTIR K, KROGAN NJ, EMRE NCT, WYCE A, THOMPSON NJ, EMILI A, HUGHES TR, GREENBLATT JF, BERGER SL (2005) H2B ubiquitin protease Ubp8 and Sgf11 constitute a discrete functional module within the Saccharomyces cerevisiae SAGA complex. *Mol Cell Biol* 25: 1162 – 1172

IVIĆ, N., GROSCHUP, B., BILOKAPIĆ, S., & HALIĆ, M. (2016). Simplified method for rapid purification of soluble histones. *Croatica chemica acta*, *89*(2), 153-162.

KAEBERLEIN, M. (2010). Lessons on longevity from budding yeast. *Nature*, 464(7288), 513-519.

KAMAKAKA, R. T., & BIGGINS, S. (2005). Histone variants: deviants? *Genes & development*, *19*(3), 295-316.

KARATHIA, H., VILAPRINYO, E., SORRIBAS, A., & ALVES, R. (2011). Saccharomyces cerevisiae as a model organism: a comparative study. *PloS one*, 6(2), e16015.

KATTYGNARATH, D., MAUGENRE, S., NEYROUD, N., BALSE, E., ICHAI, C., DENJOY, I., ... & SCHOTT, J. J. (2011). MOG1: a new susceptibility gene for Brugada syndrome. *Circulation: Cardiovascular Genetics*, 4(3), 261-268.

KIM, J., GUERMAH, M., MCGINTY, R. K., LEE, J. S., TANG, Z., MILNE, T. A., ... & ROEDER, R. G. (2009). RAD6-Mediated transcription-coupled H2B ubiquitylation directly stimulates H3K4 methylation in human cells. *Cell*, 137(3), 459-471.

KLOSE, R. J., & ZHANG, Y. (2007). Regulation of histone methylation by demethylimination and demethylation. *Nature reviews Molecular cell biology*, 8(4), 307-318.

KÖHLER A, PASCUAL-GARCÍA P, LLOPIS A, ZAPATER M, POSAS F, HURT E, RODRÍGUEZ-NAVARRO S (2006) The mRNA export factor Sus1 is involved in Spt/Ada/Gcn5 acetyltransferase-mediated H2B deubiquitinylation through its interaction with Ubp8 and Sgf11. *Mol Biol Cell* 17: 4228 – 4236

KORNBERG, R. D., & LORCH, Y. (1999). Twenty-five years of the nucleosome, fundamental particle of the eukaryote chromosome. *Cell*, 98(3), 285-294.

KOUZARIDES, T. (2007). Chromatin modifications and their function. *Cell*, 128(4), 693-705.

KROGAN NJ, DOVER J, KHORRAMI S, GREENBLATT JF, SCHNEIDER J, JOHNSTON M & SHILATIFARD A. (2002). COMPASS, a histone H3 (Lysine 4) methyltransferase required for telomeric silencing of gene expression. *J Biol Chem* 277: 10753–10755.

LAYTON, C. J., & HELLINGA, H. W. (2011). Quantitation of protein–protein interactions by thermal stability shift analysis. *Protein Science*, *20*(8), 1439-1450.

LEE, J. S., SHUKLA, A., SCHNEIDER, J., SWANSON, S. K., WASHBURN, M. P., FLORENS, L., ... & SHILATIFARD, A. (2007). Histone crosstalk between H2B monoubiquitination and H3 methylation mediated by COMPASS. *Cell*, 131(6), 1084-1096.

LEE, Y. T., GIBBONS, G., LEE, S. Y., NIKOLOVSKA-COLESKA, Z., & DOU, Y. (2015). One-pot refolding of core histones from bacterial inclusion bodies allows rapid reconstitution of histone octamer. *Protein expression and purification*, 110, 89-94.

LICHTY, J. J., MALECKI, J. L., AGNEW, H. D., MICHELSON-HOROWITZ, D. J., & TAN, S. (2005). Comparison of affinity tags for protein purification. *Protein expression and purification*, *41*(1), 98-105.

LU, J. M., DESCHENES, R. J. & FASSLER, J. S. (2004). Role for the Ran binding protein, Mog1p, in Saccharomyces cerevisiae SLN1-SKN7 signal transduction. *Eukaryotic cell*, 3(6), 1544–1556.

LUGER, K., MÄDER, A. W., RICHMOND, R. K., SARGENT, D. F., & RICHMOND, T. J. (1997a). Crystal structure of the nucleosome core particle at 2.8 Å resolution. *Nature*, 389(6648), 251.

LUGER, K., RECHSTEINER, T. J., & RICHMOND, T. J. (1999). Preparation of nucleosome core particle from recombinant histones. In *Methods in enzymology* (Vol. 304, pp. 3-19). Academic Press.

LUGER, K., RECHSTEINER, T. J., FLAUS, A. J., WAYE, M. M., & RICHMOND, T. J. (1997b). Characterization of nucleosome core particles containing histone proteins made in bacteria. *Journal of molecular biology*, *272*(3), 301-311.

MARBACH, A., & BETTENBROCK, K. (2012). lac operon induction in Escherichia coli: systematic comparison of IPTG and TMG induction and influence of the transacetylase LacA. *Journal of biotechnology*, 157(1), 82-88.

MARFATIA, K. A., HARREMAN, M. T., FANARA, P., VERTINO, P. M., & CORBETT, A. H. (2001). Identification and characterization of the human MOG1 gene. *Gene*, 266(1-2), 45-56.

MILLER, T., KROGAN, N. J., DOVER, J., ERDJUMENT-BROMAGE, H., TEMPST, P., JOHNSTON, M., ... & SHILATIFARD, A. (2001). COMPASS: a complex of proteins associated with a trithorax-related SET domain protein. *Proceedings of the National Academy of Sciences*, 98(23), 12902-12907.

MORILLON, A., KARABETSOU, N., NAIR, A., & MELLOR, J. (2005). Dynamic lysine methylation on histone H3 defines the regulatory phase of gene transcription. *Molecular cell*, *18*(6), 723-734.

MUELLER, C. L., & JAEHNING, J. A. (2002). Ctr9, Rtf1, and Leo1 are components of the Paf1/RNA polymerase II complex. *Molecular and cellular biology*, *22*(7), 1971-1980.

MUELLER, J. E., CANZE, M., & BRYK, M. (2006). The requirements for COMPASS and Paf1 in transcriptional silencing and methylation of histone H3 in Saccharomyces cerevisiae. *Genetics*, 173(2), 557-567.

NEW ENGLAND BIOLABS LNC (2011) Avoid Common Obstacles in Protein Expression. Feature Articles. Visited the 21st February 2020. Retrieved from: https://international.neb.com/tools-and-resources/feature-articles/bypassing-common-obstacles-in-protein-expression

NEW ENGLAND BIOLABS, LNC (2020). BL21(DE3) Competent E. coli. US, Visited the 15th January 2020. Retrieved from: https://www.neb.com/products/c2527-bl21de3-competent-e-coli#Product%20Information

NEW ENGLAND BIOLABS, LNC. (2019a). High Efficiency Transformation Protocol (C2987H/C2987I). Protocols. Visited the 7th June 2019. Retrieved from: https://international.neb.com/protocols/0001/01/01/high-efficiency-transformation-protocol-c2987

NEW ENGLAND BIOLABS, LNC. (2019b). Electroporation Protocol (C2989). Protocols. Visited the 10th June 2019 Retrieved from: https://international.neb.com/protocols/0001/01/01/electroporation-protocol-c2989

NG, H. H., DOLE, S., & STRUHL, K. (2003). The Rtf1 component of the Paf1 transcriptional elongation complex is required for ubiquitination of histone H2B. *Journal of Biological Chemistry*, *278*(36), 33625-33628.

NISLOW, C., RAY, E., & PILLUS, L. (1997). SET1, a yeast member of the trithorax family, functions in transcriptional silencing and diverse cellular processes. *Molecular biology of the cell*, 8(12), 2421-2436.

OKI, M., & NISHIMOTO, T. (1998). A protein required for nuclear-protein import, Mog1p, directly interacts with GTP–Gsp1p, the Saccharomyces cerevisiae Ran homologue. *Proceedings of the National Academy of Sciences*, 95(26), 15388-15393.

OLIETE-CALVO, P., SERRANO-QUÍLEZ, J., NUÑO-CABANES, C., PÉREZ-MARTÍNEZ, M. E., SOARES, L. M., DICHTL, B., ...& RODRÍGUEZ-NAVARRO, S. (2018). A role for Mog1 in H2Bub1 and H3K4me3 regulation affecting RNAPII transcription and mRNA export. *EMBO reports*, 19(11), e45992.

OSLEY, MA (2006) Regulation of histone H2A and H2B ubiquitylation. *Brief Funct Genomic Proteomic* 5: 179 – 189

OTERO, J. M., VONGSANGNAK, W., ASADOLLAHI, M. A., OLIVARES-HERNANDES, R., MAURY, J., FARINELLI, L., ... & NIELSEN, J. (2010). Whole genome sequencing of Saccharomyces cerevisiae: from genotype to phenotype for improved metabolic engineering applications. *BMC genomics*, *11*(1), 723.

PAVRI R, ZHU B, LI G, TROJER P, MANDAL S, SHILATIFARD A &REINBERG D (2006) Histone H2B monoubiquitination functions cooperatively with FACT to regulate elongation by RNA polymerase II. *Cell*, 125: 703 – 717

PETTERSEN EF, GODDARD TD, HUANG CC, COUCH GS, GREENBLATT DM, MENG EC & FERRIN TE. (2004*)* UCSF Chimera--a visualization system for exploratory research and analysis. *J Comput Chem*. Oct;25(13):1605-12.

PHIZICKY, E. M., & FIELDS, S. (1995). Protein-protein interactions: methods for detection and analysis. *Microbiol. Mol. Biol. Rev.*, *59*(1), 94-123.

RATNER, D. (1974). The interaction of bacterial and phage proteins with immobilized Escherichia coli RNA polymerase. *Journal of molecular biology*, *88*(2), 373-383.

RINAS, U., GARCIA-FRUITÓS, E., CORCHERO, J. L., VÁZQUEZ, E., SERAS-FRANZOSO, J., & VILLAVERDE, A. (2017). Bacterial inclusion bodies: discovering their better half. *Trends in biochemical sciences*, *42*(9), 726-737.

ROGUEV, A., SCHAFT, D., SHEVCHENKO, A., PIJNAPPEL, W. P., WILM, M., AASLAND, R., & STEWART, A. F. (2001). The Saccharomyces cerevisiae Set1 complex includes an Ash2 homologue and methylates histone 3 lysine 4. *The EMBO journal*, 20(24), 7137-7148.

RONDÓN, A. G., GALLARDO, M., GARCÍA-RUBIO, M., & AGUILERA, A. (2004). Molecular evidence indicating that the yeast PAF complex is required for transcription elongation. *EMBO reports*, *5*(1), 47-53.

SALARI, R., & SALARI, R. (2017). Investigation of the best Saccharomyces cerevisiae growth condition. *Electronic physician*, 9(1), 3592.

SHAH, N. B., DUNCAN, T. M. (2014). Bio-layer Interferometry for Measuring Kinetics of Protein-protein Interactions and Allosteric Ligand Effects. *J. Vis. Exp*, (84), e51383

SHAHBAZIAN M, ZHANG K & GRUNSTEIN M (2005) Histone H2B ubiquitylation controls processive methylation but not monomethylation by Dot1 and Set1. *Mol Cell* 19: 271 – 277

SHI, X., FINKELSTEIN, A., WOLF, A. J., WADE, P. A., BURTON, Z. F., & JAEHNING, J. A. (1996). Paf1p, an RNA polymerase II-associated factor in Saccharomyces cerevisiae, may have both positive and negative roles in transcription. *Molecular and cellular biology*, *16*(2), 669-676.

SHIGEKAWA, K., & DOWER, W. J. (1988). Electroporation of eukaryo and prokaryotes: a general approach to the introduction of macromolecules into cells. *Biotechniques*, 6(8), 742-751.

SHILATIFARD A. (2012). The COMPASS family of histone H3K4 methylases: Mechanisms of regulation in development and disease pathogenesis. *Annu Rev Biochem* 81: 65–95.

SHIM, Y., DUAN, M. R., CHEN, X., SMERDON, M. J., & MIN, J. H. (2012). Polycistronic coexpression and nondenaturing purification of histone octamers. *Analytical biochemistry*, *427*(2), 190-192.

SHUKLA A, STANOJEVIC N, DUAN Z, SHADLE T& BHAUMIK SR (2006) Functional analysis of H2B-Lys-123 ubiquitination in regulation of H3-Lys- 4 methylation and recruitment of RNA polymerase II at the coding sequences of several active genes in vivo. *J Biol Chem* 281: 19045 – 19054

SIKORSKI, R. S., & HIETER, P. (1989). A system of shuttle vectors and yeast host strains designed for efficient manipulation of DNA in Saccharomyces cerevisiae. *Genetics*, 122(1), 19-27.

SMITS, J. P., ECKARDT, L., PROBST, V., BEZZINA, C. R., SCHOTT, J. J., REMME, C. A., ... & LEMAREC, H. (2002). Genotype-phenotype relationship in Brugada syndrome: electrocardiographic features differentiate SCN5A-related patients from non–SCN5A-related patients. *Journal of the American College of Cardiology*, *40*(2), 350-356.

SOARES LM & BURATOWSKI S. (2012). Yeast Swd2 is essential because of antagonism between Set1 histone methyltransferase complex and APT (associated with Pta1) termination factor. *J Biol Chem* 287: 15219–15231.

SOME, D. (2013). Light-scattering-based analysis of biomolecular interactions. *Biophysical reviews*, 5(2), 147-158.

SQUAZZO, S. L., COSTA, P. J., LINDSTROM, D. L., KUMER, K. E., SIMIC, R., JENNINGS, J. L., ... & HARTZOG, G. A. (2002). The Paf1 complex physically and functionally associates with transcription elongation factors in vivo. *The EMBO journal*, *21*(7), 1764-1774.

STEGGERDA, S. M., & PASCHAL, B. M. (2000). The mammalian Mog1 protein is a guanine nucleotide release factor for Ran. *Journal of Biological Chemistry*, *275*(30), 23175-23180.

STEGGERDA, S. M., & PASCHAL, B. M. (2001). Identification of a conserved loop in Mog1 that releases GTP from Ran. *Traffic*, 2(11), 804-811.

STEPHENS, D. J., & BANTING, G. (2000). The use of yeast two-hybrid screens in studies of protein: Protein interactions involved in trafficking. *Traffic*, *1*(10), 763-768.

STEWART, M., & BAKER, R. P. (2000). 1.9 Å resolution crystal structure of the Saccharomyces cerevisiae Ran-binding protein Mog1p. *Journal of molecular biology*, 299(1), 213-223.

SWANEY, D. L., BELTRAO, P., STARITA, L., GUO, A., RUSH, J., FIELDS, S., ... & VILLÉN, J. (2013). Global analysis of phosphorylation and ubiquitylation cross-talk in protein degradation. *Nature methods*, *10*(7), 676.

SYNTHETIC YEAST 2.0 (2020) Science across Virtual Institutes (SAVI). Visited the 7th February 2020. Retrieved from: http://syntheticyeast.org/

TAKARA BIO LNC (2018) Batch or gravity-flow purification of his-tagged proteins-TALON Metal Affinity Resin. Takara. Visited the 18th February 2020. Retrieved from: https://www.takarabio.com/products/protein-research/purification-products/his-tagged-protein-purification/bulk-resins-and-gravity-columns/cobalt-resin

TANAKA, Y., TAWARAMOTO-SASANUMA, M., KAWAGUCHI, S., OHTA, T., YODA, K., KURUMIZAKA, H., & YOKOYAMA, S. (2004). Expression and purification of recombinant human histones. *Methods*, 33(1), 3-11.

TATEBAYASHI, K., TANI, T., & IKEDA, H. (2001). Fission yeast Mog1p homologue, which interacts with the small GTPase Ran, is required for mitosis-to-interphase transition and poly (A)+ RNA metabolism. *Genetics*, 157(4), 1513-1522.

THERMOSCIENTIFIC (2019). Phusion™ Site Directed Mutagenesis Kit. Catalogue Number F541. Thermoscientific User guide. Visited the 7th June 2019. Retrieved from: https://assets.thermofisher.com/TFSAssets/LSG/manuals/MAN0013377_Phusion_SiteDirected_Mutagenesis_UG.pdf

THORNTON, J. L., WESTFIELD, G. H., TAKAHASHI, Y. H., COOK, M., GAO, X., WOODFIN, A. R., ... & COUTURE, J. F. (2014). Context dependency of Set1/COMPASS-mediated histone H3 Lys4 trimethylation. *Genes & development*, *28*(2), 115-120.

TRUJILLO KM &OSLEY MA (2012) A role for H2B ubiquitylation in DNA replication. *Mol Cell* 48: 734 – 746

UNIPROT CONSORTIUM (2019). UniProt: a worldwide hub of protein knowledge. *Nucleic acids research*, *47*(D1), D506-D515.

URBAN, M. K., FRANKLIN, S. G., & ZWEIDLER, A. (1979). Isolation and characterization of the histone variants in chicken erythrocytes. *Biochemistry*, *18*(18), 3952-3960.

VAN OSS, S. B., SHIRRA, M. K., BATAILLE, A. R., WIER, A. D., YEN, K., VINAYACHANDRAN, V., ... & KIM, J. (2016). The histone modification domain of Paf1 complex subunit Rtf1 directly stimulates H2B ubiquitylation through an interaction with Rad6. *Molecular cell*, *64*(4), 815-825.

VITALIANO-PRUNIER A, BABOUR A, HÉRISSANT L, APPONI L, MARGARITIS T, HOLSTEGE FCP, CORBETT AH, GWIZDEK C, DARGEMONT C (2012) H2B ubiquitylation controls the formation of export-competent mRNP. *Mol Cell* 45: 132 – 139

VITALIANO-PRUNIER, A., MENANT, A., HOBEIKA, M., GÉLI, V., GWIZDEK, C., & DARGEMONT, C. (2008). Ubiquitylation of the COMPASS component Swd2 links H2B ubiquitylation to H3K4 trimethylation. *Nature cell biology*, *10*(11), 1365-1371.

VLAMING, H., & VAN LEEUWEN, F. (2016). The upstreams and downstreams of H3K79 methylation by DOT1L. *Chromosoma*, *125*(4), 593-605.

WALLIS, J. W., HEREFORD, L., & GRUNSTEIN, M. (1980). Histone H2B genes of yeast encode two different proteins. *Cell*, 22(3), 799-805.

WANG, H., WANG, L., ERDJUMENT-BROMAGE, H., VIDAL, M., TEMPST, P., JONES, R. S., & ZHANG, Y. (2004). Role of histone H2A ubiquitination in Polycomb silencing. *Nature*, 431(7010), 873.

WEAKE VM & WORKMAN JL (2008) Clearing the way for unpaused polymerases. *Cell* 134: 16 – 18

WINSTON, F., DOLLARD, C., & RICUPERO-HOVASSE, S. L. (1995). Construction of a set of convenient Saccharomyces cerevisiae strains that are isogenic to S288C. *Yeast*, 11(1), 53-55.

WITTIG, I., BRAUN, H. P., & SCHÄGGER, H. (2006). Blue native PAGE. *Nature protocols*, *1*(1), 418.

WOOD A, SCHNEIDER J, DOVER J, JOHNSTON M, SHILATIFARD A (2003) The Paf1 complex is essential for histone monoubiquitination by the Rad6-Bre1 complex, which signals for histone methylation by COMPASS and Dot1p. *J Biol Chem* 278: 34739 – 34742

WOOD, W. B. (1966). Host specificity of DNA produced by Escherichia coli: bacterial mutations affecting the restriction and modification of DNA. *Journal of molecular biology*, 16(1), 118-IN3.

WU, L., YONG, S. L., FAN, C., NI, Y., YOO, S., ZHANG, T., ... & SZAFRANSKI, P. (2008). Identification of a new co-factor, MOG1, required for the full function of cardiac sodium channel Nav1. 5. *Journal of Biological Chemistry*, *283*(11), 6968-6978.

YAMAGUCHI, H., & MIYAZAKI, M. (2014). Refolding techniques for recovering biologically active recombinant proteins from inclusion bodies. *Biomolecule*s, 4(1), 235-251.

YU, G., LIU, Y., QIN, J., WANG, Z., HU, Y., WANG, F., ... & WANG, Q. K. (2018). Mechanistic insights into the interaction of the MOG1 protein with the cardiac sodium channel Nav1. 5 clarify the molecular basis of Brugada syndrome. *Journal of Biological Chemistry*, *293*(47), 18207-18217.

ZHENG S, WYRICK JJ & REESE JC. (2010). Novel trans-tail regulation of H2B ubiquitylation and H3K4 methylation by the N terminus of histone H2A. *Mol Cell Biol* 30: 3635–3645.

8.APPENDIX

8.1. Creation of the double mutant *set1Δmog1Δ* from *set1Δ* strain

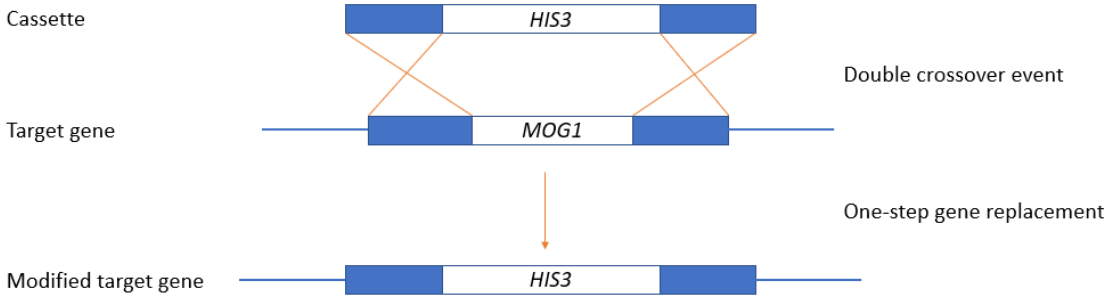

Figure 8.1. *MOG1* disruption by PCR amplified *HIS3* cassette. *MOG1* deletion takes place by a double crossover event during homologous recombination. The homologous regions flanking both *MOG1* and *HIS3* are 40nt length.

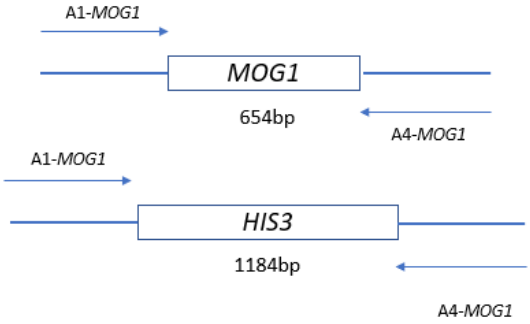

Figure 8.2. PCR amplification of the modified target gene. Primers designed to align to the flanking regions of the target gene allow the detection of the gene disruption due to difference in size between the target gene and the selection marker.

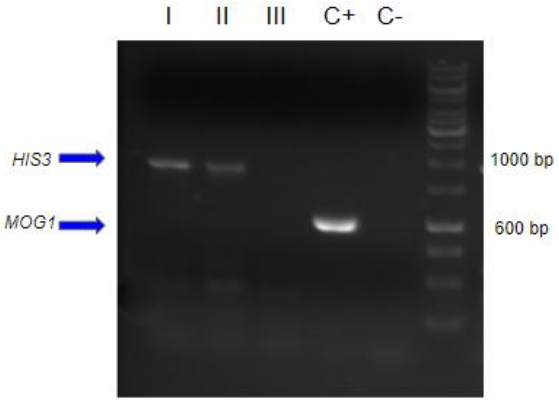

Figure 8.3. Confirmation of *MOG1* deletion in *set1Δ*. 1% agarose gel electrophoresis of the PCR products from the *HIS3/MOG1* amplification in the three clones transformed with *HIS3*::*MOG1*. As the positive control, the DNA from a non-transformed *set1Δ* colony was used while the negative control corresponded to the PCR mix without DNA.

8.2. Phenotypic effect of Mog1ΔK144-T153 and Mog1K189A mutations in *mog1Δ* and *set1Δmog1Δ S. cerevisiae* growth

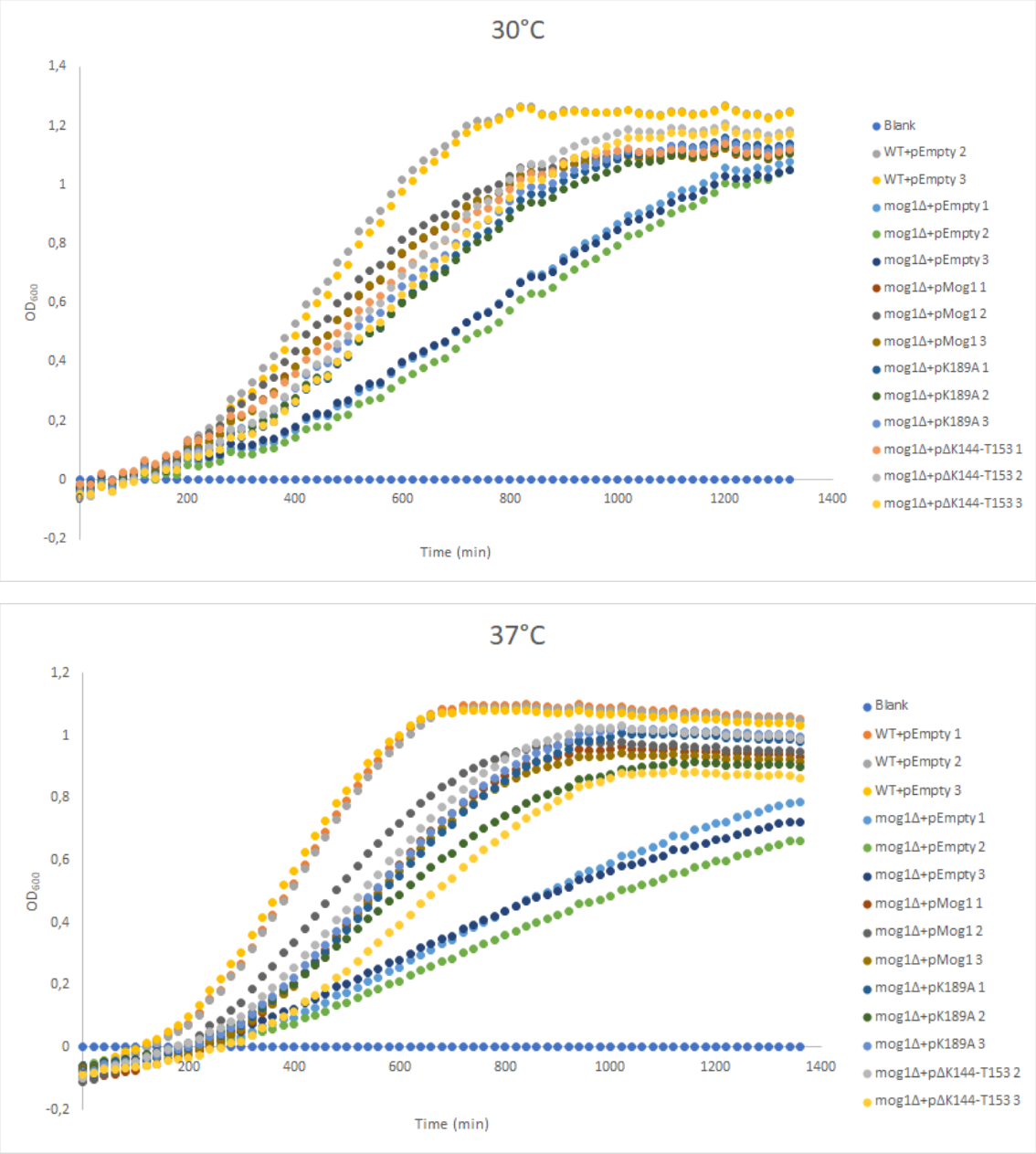

Figure 8.4. Growth curves of the WT/*mog1Δ* strains represented as OD_{600} vs. time. WT+pEmpty replicate 1 (30ºC) and *mog1Δ*+pΔK144-T153 replicate 1 (37ºC) were removed from the data set and not included in further analysis because of significant deviation from their replicates. Blank values corresponded to the OD_{600} measurements of the growth media SC-Leu and were used to normalise the OD_{600} values at each time point.

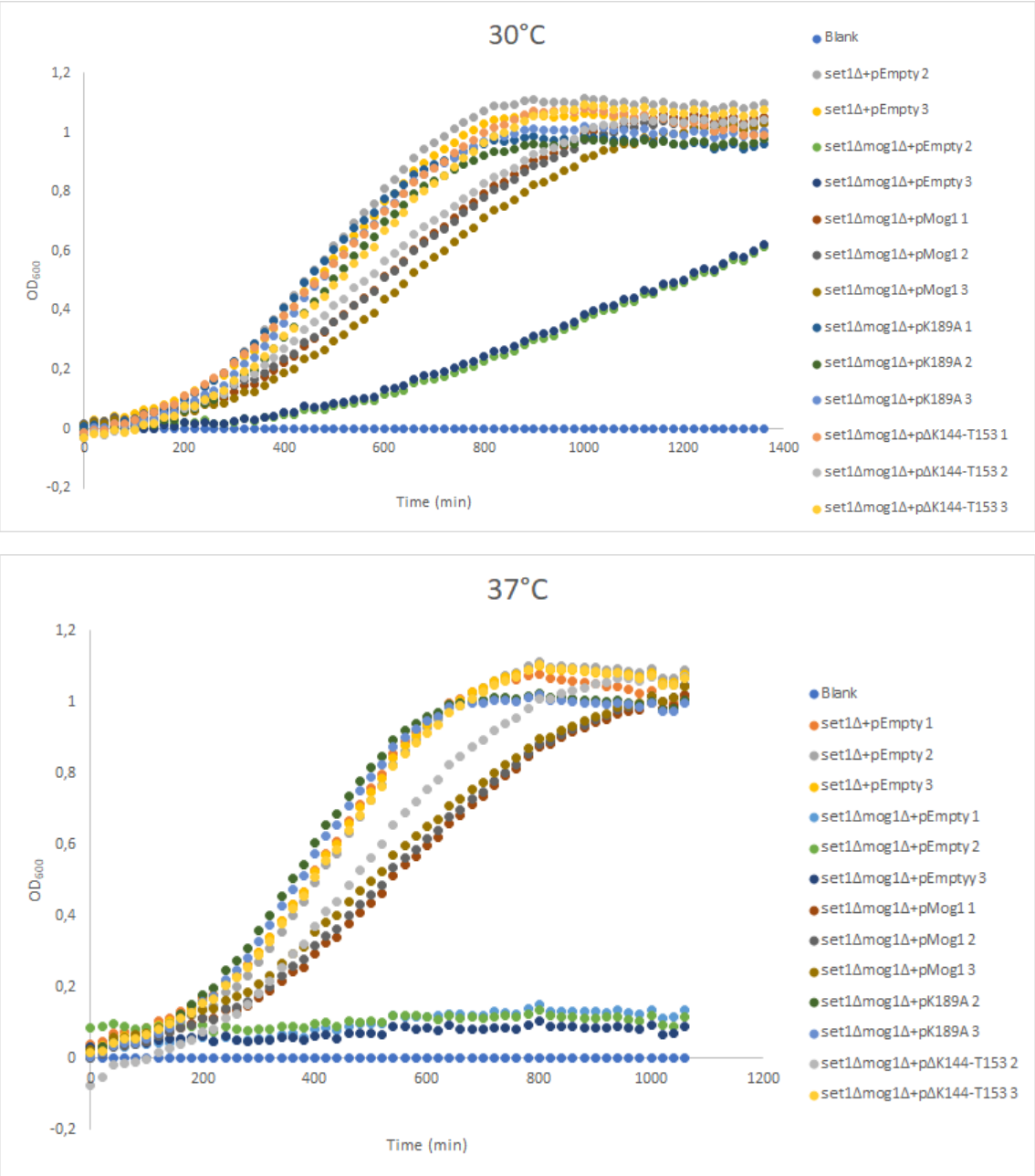

Figure 8.5. Growth curves of the *set1Δ*/*set1Δmog1Δ* strains represented as OD_{600} vs. time. *set1Δ*+pEmpty replicate 1 (30ºC), *set1Δmog1Δ*+pEmpty replicate 1 (30ºC), *set1Δmog1Δ*+pK189A replicate 1 (37ºC) and *set1Δmog1Δ*+pΔK144-T153 replicate 1 (37ºC) were removed from the data set and not included in further analysis because of significant deviation amongst their replicates. Blank values corresponded to the OD_{600} measurements of the growth media SC-Leu and were used to normalise the OD_{600} values at each time point.

Table 8.1. Growth rates and doubling times calculated from the exponential phase of the growth curves in Appendix, Figures 8.4 and 8.5. The values shown in the table correspond to the average of the growth rate and doubling time calculated for each of the replicates of the indicated strains

	GROWTH RATE (min^{-1})		DUPLICATION TIME (min)	
Strain	30°C	37°C	30°C	37°C
WT+pEmpty	0.0043	0.0043	161.28	163.12
mog1Δ+pEmpty	0.0020	0.0017	341.07	401.13
mog1Δ+pMog1	0.0036	0.0035	191.00	196.32
mog1Δ+pK189A	0.0032	0.0031	217.17	226.41
mog1Δ+pΔK144-T153	0.0034	0.0033	206.17	214.55
set1Δ+pEmpty	0.0032	0.0037	216.82	189.94
set1Δmog1Δ+pEmpty	0.0016	0.0000	447.66	0.00
set1Δmog1Δ+pMog1	0.0026	0.0028	263.30	244.71
set1Δmog1Δ+pK189A	0.0031	0.0038	223.75	182.53
set1Δmog1Δ+pΔK144-T153	0.0029	0.0035	236.55	201.97

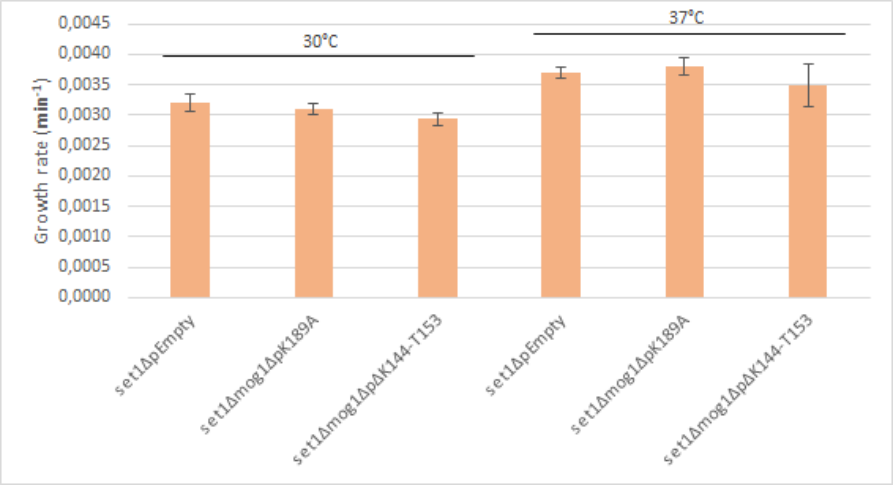

Figure 8.6 Growth rate values of *set1Δmog1Δ*+pK189A and *set1Δmog1Δ*+ pΔK144-T153 compared to *set1Δ*+pEmpty at 30ºC and 37ºC. The lines above the bars indicate the strains included in each ANOVA analysis which were then compared to *set1Δ*+pEmpty in pairs by t-test at each condition. None of the *set1Δmog1Δ*+pK189A and *set1Δmog1Δ*+ pΔK144-T153 showed significantly different growth rates compared to *set1Δ*+pEmpty.

8.3. IPTG induced expression of His-tagged H2B and purification by IMAC

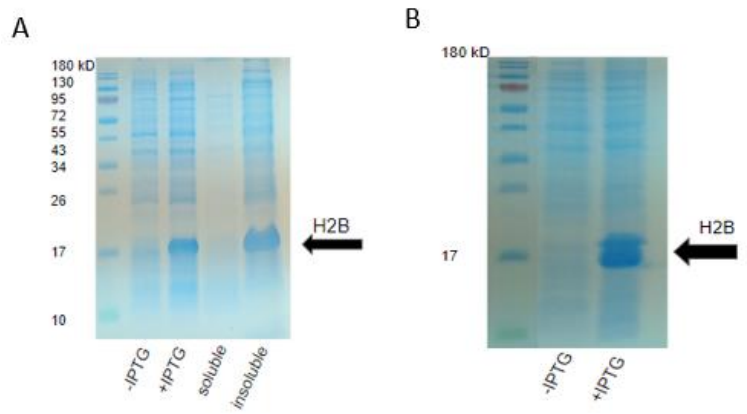

Figure 8.7. H2B induced expression test with 1mM IPTG at 4ºC for 3h. A) from 10ml LB+Chl+Kan. B) from 1L+Chl+Kan 15% SDS-PAGE gel for testing IPTG induced expression of H2B comparing samples before and after addition of 1mM IPTG together with soluble and insoluble fractions of the IPTG induced cell extract.

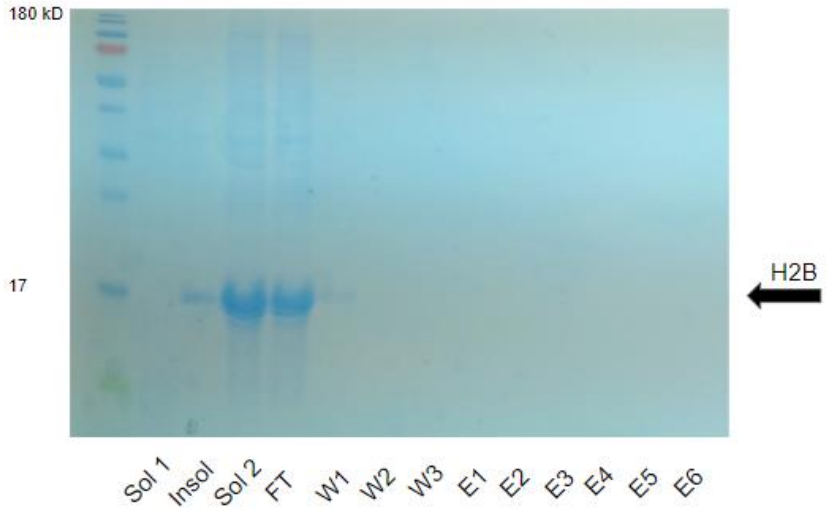

Figure 8.8. H2B purification with TALON column under denaturing conditions. The insoluble fraction of the cell extract was resuspended in washing buffer containing 8M urea and applied to the column containing TALON beads. Apart from the solubilised fraction (Sol 2), flow through (FW), washing (W1-3) and elution samples (E1-6), samples from the soluble fraction (Sol 1) and the insoluble fraction before solubilization in denaturing conditions (Insol) were also run in the gel to check solubilisation of H2B.

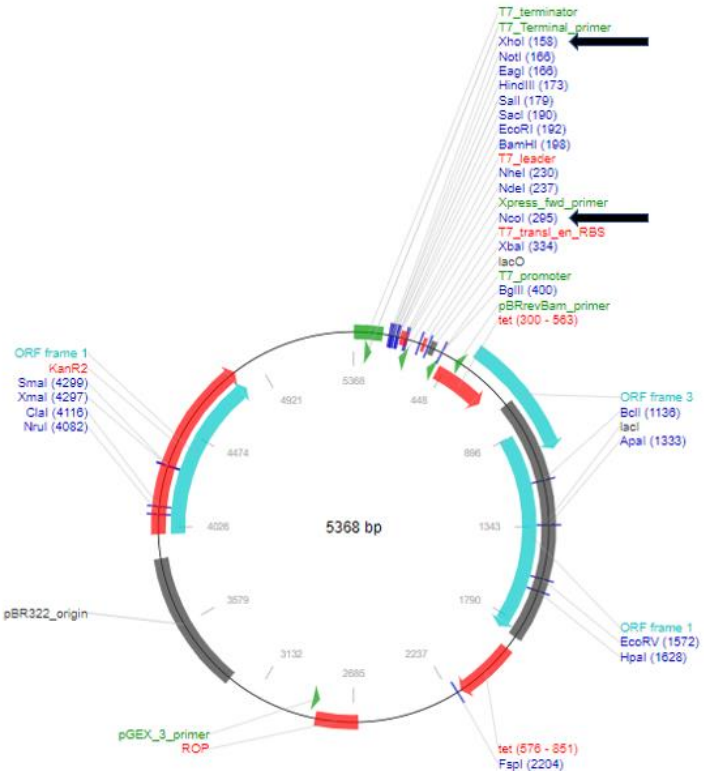

Figure 8.9. Map of the pET28b plasmid from ADDGENE (2019). The arrows indicate the cloning sites of *HTB1*.

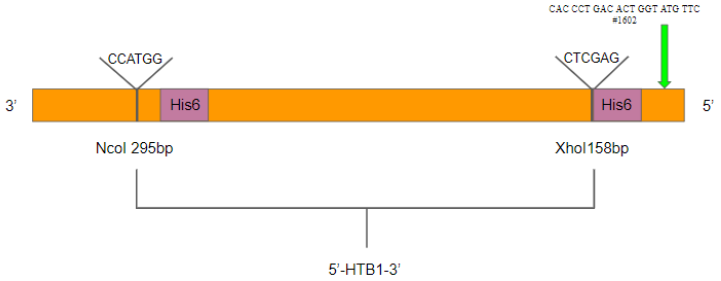

Figure 8.10. Cloning site of *HTB1* gene in pET28b plasmid. *A3-HTB1* 21bp primer designed to sequence from the 3' terminal of *HTB1* (Materials and Methods, Table 3.6), anneals 100bp away the 3' terminal.

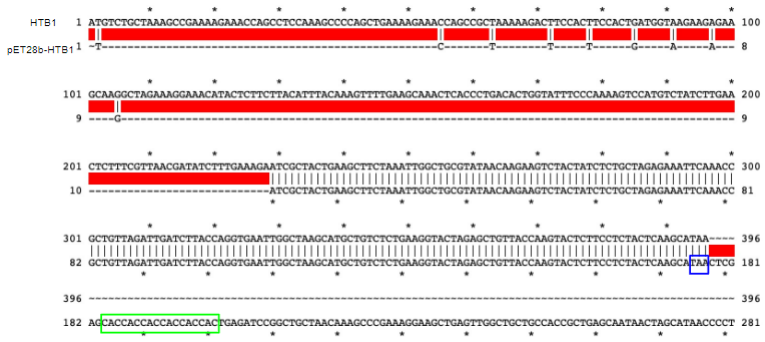

Figure 8.11. Local alignment of the *HTB1* gene sequence to the fragment of pET28b-*HTB1* sequenced using the primer named A3-*HTB1* (Materials and Methods, Table 3.6). The sequence on top corresponds to *HTB1* gene and the bottom sequence to the results of sequencing. Highlighted in blue the stop codon present in the *HTB1* gene cloned into pET28b and in green the His6-tag sequence at the 3' end of the gene.

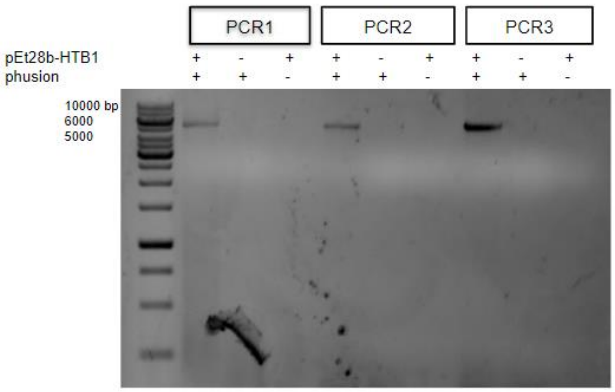

Figure 8.12. Deletion of the stop codon from the pET28b-*HTB1* plasmid by quick-change. PCR1: HF Phusion buffer® as the Taq polymerase buffer; PCR2: HF Phusion buffer® and 5% DMSO added to the transformation mix; PCR3: GC Phusion buffer® as the Taq polymerase buffer. Two negative controls for each condition: PCR negative control (without plasmid) and mutagenesis negative control (without Phusion polymerase). Samples were run in a 1% agarose gel with a 1kB marker.

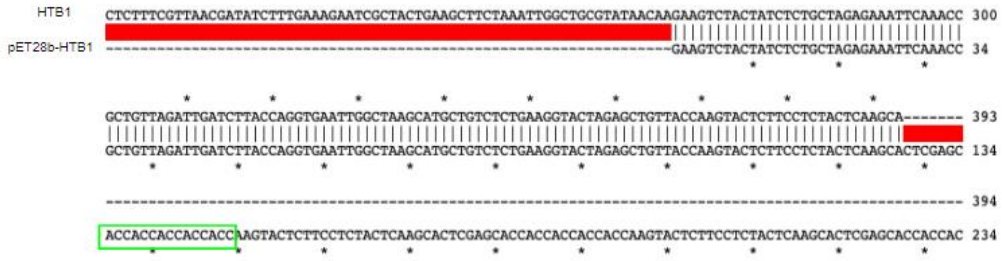

Figure 8.13. Local alignment of the *HTB1* gene sequence to the fragment of pET28b-*HTB1* sequenced using the primer named A4-pET28b (Materials and Methods, Table 3.6). The sequence on top corresponds to *HTB1* gene and the bottom sequence to the fragment of pET28b-*HTB1* Sequenced. Highlighted in green the His6-tag sequence at the 3' end of the gene. The stop codon has been successfully deleted.

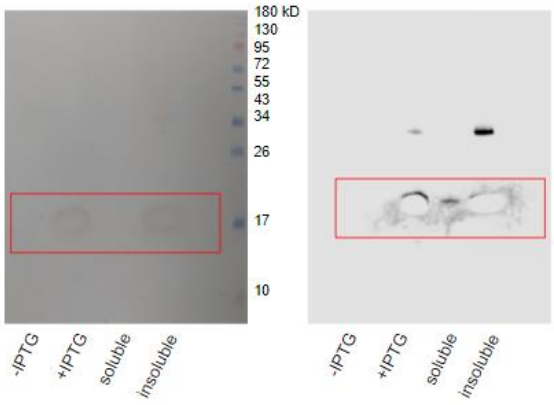

Figure 8.14. Expression of the His6 tag detected by transfer and immunoblotting of His6-tagged *HTB1*. The images show the membrane before (left) and after (right) being revealed in a luminescent image analyser. Membrane burnt because of high expression of the histidine tail.